Advanced Drug Delivery Reviews 72 (2014) 65–81

Contents lists available at ScienceDirect

Advanced Drug Delivery Reviews

journal homepage: www.elsevier.com/locate/addr

Magnetic resonance guided high-intensity focused ultrasound for image-guided temperature-induced drug delivery ☆

Nicole Hijnen [a,c], Sander Langereis [b,c], Holger Grüll [a,b,c,*]

[a] Eindhoven University of Technology, Dept. of Biomedical NMR, Eindhoven, The Netherlands
[b] Philips Research Eindhoven, Minimally Invasive Healthcare, Eindhoven, The Netherlands
[c] Center for Imaging Research and Education (CIRE), Eindhoven, The Netherlands

ARTICLE INFO

Available online 22 January 2014

Keywords:
Drug delivery
MR-HIFU
Temperature-sensitive liposomes
Ultrasound
MR image guidance
Doxorubicin

ABSTRACT

Magnetic resonance guided high-intensity focused ultrasound (MR-HIFU) is a versatile technology platform for noninvasive thermal therapies in oncology. Since MR-HIFU allows heating of deep-seated tissue to well-defined temperatures under MR image guidance, this novel technology has great potential for local heat-mediated drug delivery from temperature-sensitive liposomes (TSLs). In particular, MR provides the ability for image guidance of the drug delivery when an MRI contrast agent is co-encapsulated with the drug in the aqueous lumen of the liposomes. Monitoring of the tumor drug coverage offers possibilities for a personalized thermal treatment in oncology. This review focuses on MR-HIFU as a noninvasive technology platform, temperature-sensitive liposomal formulations for drug delivery and image-guided drug delivery, and the effect of HIFU-induced hyperthermia on the TSL and drug distribution. Finally, the opportunities and challenges of localized MR-HIFU-mediated drug delivery from temperature-sensitive liposomes in oncology are discussed.

Contents

1. Introduction

Recent developments in medical technologies and new insights into cancer biology have advanced cancer care considerably with improved cure rates and extended life expectancies [1]. Yet, the challenge in chemotherapy to achieve sufficient drug levels in the tumor, while reducing off-site drug uptake, remains largely unresolved. Typically, chemotherapeutic drugs are systemically administered and only a small percentage of the drug reaches the cancerous lesion, while the majority of the drug is cleared or taken up in healthy organs causing undesired side effects. The therapeutic window for a drug treatment regimen is defined by the drug doses that achieve the highest therapeutic efficacy while keeping the side effects manageable and tolerable. Consequently, research has been devoted to drug delivery approaches using larger drug conjugates or drug loaded nanoparticles that afford

☆ This review is part of the *Advanced Drug Delivery Reviews* theme issue on "Ultrasound triggered drug delivery".

* Corresponding author at: Dept. Biomedical NMR, Eindhoven University of Technology, Den Dolech 2, 5600 MB Eindhoven, The Netherlands.
E-mail address: h.gruell@tue.nl (H. Grüll).

0169-409X/$ – see front matter © 2014 Elsevier B.V. All rights reserved.
http://dx.doi.org/10.1016/j.addr.2014.01.006

higher drug concentrations in the tumor while decreasing off-site toxicity [2–6]. For instance, chemotherapeutic drugs have been encapsulated in the lumen of liposomes, which prevents the rapid extravasation of the small parental drug (size ca. 1 nm) into healthy tissue [7–9]. Upon injection, these long circulating liposomal drug carriers are taken up in the tumor mediated by the enhanced permeability and retention (EPR) effect, which is a characteristic of angiogenic blood vessels in neoplasms [10–13]. These permeable blood vessels with gaps in the endothelial lining allow extravasation of macromolecules or nanoparticles into the interstitial space that would otherwise stay intravascular [14,15]. The EPR effect has been exploited in passive targeting of tumors using nanoparticulate drug formulations as well as macromolecular drug conjugates in a plethora of preclinical studies [10,16–18]. In the clinical practice, however, this approach has its limitations as the EPR effect is less pronounced in the commonly slower growing human tumors compared to more aggressive tumors used in preclinical models [19]. Furthermore, liposomal drug encapsulation reduces drug uptake in healthy tissue, but at the same time hampers the bioavailability of the parent drug in the tumor. An alternative strategy that may overcome the aforementioned disadvantages was suggested by Yatvin and Weinstein by proposing temperature-sensitive liposomes (TSLs) for drug delivery [20,21]. Here, the drug remains encapsulated in the aqueous lumen of the TSL at body temperature, but releases the drug from the TSL at hyperthermic temperatures in the range of 40–45 °C [22]. The applicability of drug loaded TSLs in oncology requires accurate heating of the targeted lesion in a controlled and preferably noninvasive manner to stable hyperthermic conditions over a period of ca. 30 min to 1 h. Temperature-triggered drug delivery has been tested in a plethora of preclinical studies and has reached the clinical trial phase for several applications in oncology, such as radiofrequency (RF) ablation of hepatocellular carcinoma (HCC) primary liver tumors, liver metastasis, and recurrent chest wall breast cancer [23–27].

Local heating can be established with radiofrequency, light, water bath, and ultrasound, each with its pros and cons with respect to possible applications [28]. Diagnostic imaging modalities like computed tomography (CT), X-ray, ultrasound and magnetic resonance imaging (MRI) play a crucial role for planning of the procedure and providing spatial guidance to reach the targeted tissue [29]. For example, the insertion of interstitial RF ablation needles is planned based on CT information and performed under X-ray or ultrasound guidance to ensure optimal coverage of the targeted lesion. For regional hyperthermia applications using extracorporeal RF applicators, MRI plays an increasing role during the planning phase, and during the hyperthermia treatment to provide spatial guidance and near real-time *in vivo* temperature information [30–35]. The strength of MRI in providing spatial, temporal, and temperature feedback is fully exploited in devices integrating a high-intensity focused ultrasound (HIFU) transducer within the patient bed of an MRI scanner (MR-HIFU). As HIFU allows to heat tissue noninvasively providing an acoustic beam path is present, the entire workflow from diagnosis, planning, guidance of the HIFU procedure and immediate therapy assessment can be performed on one platform (Fig. 1). Currently, the main clinical application of MR-HIFU is thermal ablation of uterine fibroids, a benign smooth muscle tumor [36–39]. The clinical use of MR-HIFU is expanding to pain palliation in bone metastasis [40]. Further clinical testing is ongoing for the treatment of essential tremor [41], and the ablation of breast and prostate cancers [42,43]. As MR-HIFU allows maintaining constant temperatures over an extended period of time, this platform has been recognized as a potential technology solution for hyperthermia applications.

Hyperthermia is well-established as a sensitizer for chemo- and radiation therapy [44,45]. While temperatures higher than 43 °C contribute directly to thermotoxicity, mild hyperthermia (39–42 °C) acts synergistically with chemo- and radiotherapy on a tissue and cellular level [45–48]. On a cellular level, hyperthermia alters biological pathways, making the cell more susceptible to radiation and chemically-induced cytotoxicity [49]. On tissue and organ level, mild hyperthermia increases blood flow and enhances oxygenation, which is an important enhancer of radiotherapy [50]. Hyperthermia-induced increase of the vascular permeability improves delivery of therapeutic agents to the tumor tissue [51]. The benefit for combined thermochemo- and

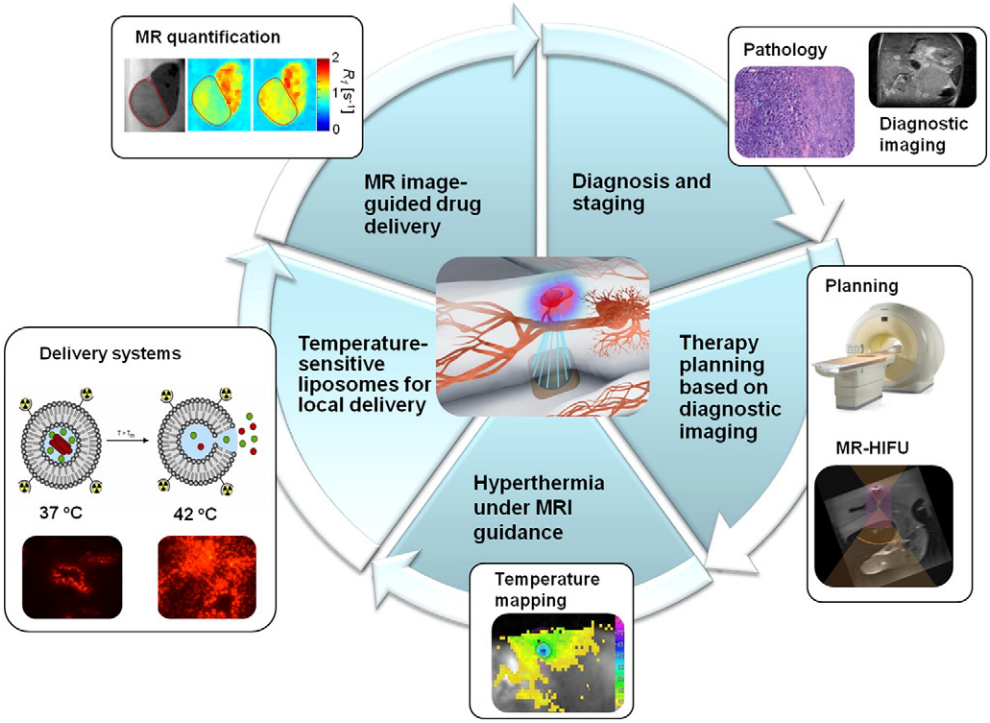

Fig. 1. MR-HIFU: a versatile technology platform for thermal therapy. MR guidance plays a pivotal role in diagnosis, planning, monitoring, and assessment of the therapy. Near real-time MR temperature mapping provides feedback on the well-defined, spatially controlled HIFU heating. Furthermore, MR image-guided drug delivery employing image-able TSLs allows the estimation of the drug coverage of the heated tissue.

thermoradiotherapy has been demonstrated in major clinical studies [52–56]. However, the temperature window for successful hyperthermia applications is narrow, as therapeutic outcome has been shown to depend on the exact thermal dose that has been delivered over the course of treatment [57–61]. Moreover, vascular shutdown can occur when a critical temperature of ca. 43 °C is exceeded, which is detrimental for adjunct chemo- and radiotherapeutic treatments [62,63]. MR-HIFU offers the perspective of a versatile technology platform that allows accurate temperature control for clinical application of hyperthermia. The tight temperature control and MR image guidance make MR-HIFU an ideal candidate for temperature-induced image-guided drug delivery from TSLs co-encapsulating a drug and an MRI contrast agent. The latter allows *in vivo* visualization and quantification of the drug dose delivered to the tumor, which may be used for a more personalized approach in cancer therapy.

This review will focus on MR-HIFU as a noninvasive technology platform for thermal therapy in oncology. MR-HIFU for thermal ablation and hyperthermia-mediated local drug delivery using temperature-sensitive liposomes will be addressed. In particular, the effect of HIFU-induced hyperthermia on the pharmacokinetics of the TSL and the parent drug will be highlighted.

2. MR-HIFU technology for noninvasive thermal therapy

High-intensity focused ultrasound (HIFU) is a promising technology for controlled, noninvasive tumor treatment by selective tissue heating [35,64–67]. By focusing the mechanical ultrasound waves, ultrasonic energy can be deposited deep within the body without harming surrounding tissue, causing a fast and local temperature rise. Tissues can be heated to temperatures considerably above body temperature, which can be used for direct thermal ablation of lesions. Coagulative necrosis sets in above a certain thermal dose, which shows an Arrhenius-type time–temperature dependence [68]. Although focused ultrasound for local tissue destruction was recognized in the 1940s, the technology did not gain widespread clinical acceptance due to lack of spatial guidance. In the late 1980s, treatment guidance using diagnostic ultrasound imaging provided a method for identification of the target volume, analysis of the acoustical pathway, and for real-time tissue information [69–71]. Magnetic resonance image guidance of the HIFU treatment (MR-HIFU) further accelerated the clinical application as the MRI not only provided excellent soft tissue contrast that can be exploited for precise treatment planning and immediate treatment follow-up, it also offered the ability to visualize the HIFU-induced temperature changes using MR thermometry [72–74]. Accurate temperature monitoring and feedback is of critical importance during thermal treatments as the therapeutic effect largely depends on the actual temperature rise that is obtained in the target tissue. As various tissue layers differ in their ultrasound absorption coefficients and scattering as well as in heat diffusion and tissue perfusion, a prediction of the actual temperature distribution in the target tissue and its surroundings based on the ultrasound settings is difficult to make. Furthermore, reproducibility and standardization of the treatment is complex without taking into account the complete thermal history during the treatment (*i.e.* dose information). From the different MR thermometry techniques available [74], proton resonance frequency shift (PRFS) MR thermometry is by far the most commonly used in water-containing tissues, providing a temperature precision of approximately 1 °C [72,75,76]. With the spatial and temporal temperature feedback provided by the MR thermometry guidance, closed-loop, innovative MR-HIFU systems have been developed (Fig. 2). Next to fast heating to a predefined temperature for thermal ablation purposes, the constant temperature feedback allowed us to maintain a certain temperature for a prolonged time period by dynamic adjustment of the sonication parameters. The latter feature of the MR-HIFU technology platform can be exploited for noninvasive, targeted hyperthermia treatments [77].

The strength of MR-HIFU is accurate delivery of a high thermal dose to a pre-defined volume in a noninvasive manner. Traditionally, HIFU heating has been performed by iteratively sonicating a single focal point at a time with each sonication followed by a cooling period. This approach allowed simultaneous heating of small tissue volumes (*i.e.* the size of a single focal spot which typically approximates $1 \times 1 \times 9$ mm^3) and was very time consuming for the treatment of larger volumes. Technological developments in the transducer design significantly improved the efficacy of MR-HIFU by making use of multi-element phased array transducers. The phased array design allows for the creation of different focal patterns and electronic steering of the foci by adjusting the relative phase and magnitude of the acoustic waves generated by each transducer element [78,79]. Furthermore, the electronic steering capabilities of the phased array design shortened the treatment time by reducing the need for mechanical movement of the transducer during the sonication [78,80].

Cylindrical section ultrasound phased array transducers have been proposed for larger volume hyperthermia (*e.g.* $50 \times 50 \times 30$ mm^3) [82], however, this configuration was not compatible with MR guidance. An energy efficient method for homogeneous ultrasound heating of tissue volumes up to 16 mm in diameter (treatment volume = $16 \times 16 \times 25$ mm^3) under MR guidance was proposed by Köhler et al. [81]. The focal spot was electronically steered around multiple concentric outward-moving circles, making optimal use of heat diffusion. Such a volumetric heating approach has been implemented on clinical MR-HIFU systems (Sonalleve®, Philips Healthcare) (Fig. 2). Moreover, protocols for MR-HIFU mediated hyperthermia over a prolonged period of time have been developed based on a binary feedback control algorithm that switches the transducer power on or off at predefined threshold temperatures [83,84]. This method has been demonstrated for hyperthermia and hyperthermia-induced drug delivery in rat [83,85] and rabbit models [86–88]. In a preclinical setting, HIFU-induced hyperthermia has been studied mainly in small tumor volumes with typical diameters of max. 2 cm. With these tumor sizes, heat diffusion ensures sufficient heating of the tissue surrounding the tumor. However, for clinical hyperthermia applications, either in combination with radio- or (local) chemotherapy, larger volumes (range of 3–8 cm) need to be covered.

A sonication approach using multiple concurrent foci might be used for large-volume hyperthermia with a clinical MR-HIFU device [89]. In this case, the multi-foci sonication approach minimizes the risk for mechanical tissue damage. MR-HIFU-mediated hyperthermia methods for large volume (up to approximately 5 cm in diameter), for example, by switching between several volumetric heating cells using multiple transducer positions, are currently investigated. With these technological developments, MR-HIFU will evolve into a generic technology platform for thermal therapies comprising local hyperthermia as a sensitizer of radio- and chemotherapy, hyperthermia triggered-drug delivery and thermal ablation of tumor tissue. Other existing technology solutions for invasive and non-invasive heating provide solutions for *e.g.* regional hyperthermia or large area superficial hyperthermia (Fig. 3). The choice of the most suited heating technology depends on the size of the targeted lesion and its exact location, for example, the presence of vulnerable and crucial structures that need to be spared.

3. Liposomal formulations for temperature-induced drug delivery

The advantages of temperature-sensitive liposomes (TSLs) for temperature-induced drug delivery are the enhanced drug uptake at the tumor site and decreased drug toxicity profiles in healthy tissue as compared to the systemic administration of low molecular weight parent drugs. The design criteria of the TSLs depend on the heating strategy used (*i.e.* intra- or extravascular release). In general, the TSLs should: (*i*) stably encapsulate the drug in the aqueous compartment at body temperature; (*ii*) provide a rapid and quantitative release at hyperthermic temperature; and (*iii*) provide high drug plasma levels during the time span of hyperthermia treatment.

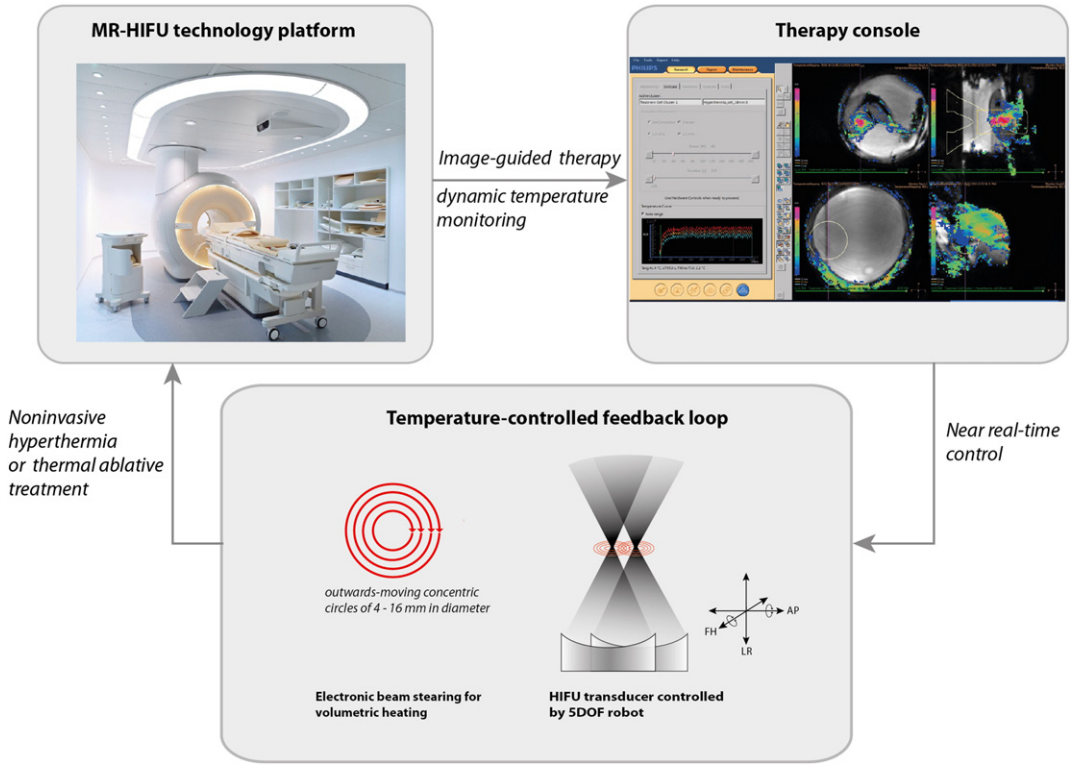

Fig. 2. MR-HIFU system (Sonalleve®, Philips Healthcare) designed for the thermal ablation treatment of uterine fibroids. A phased array ultrasound transducer containing 256 separate elements is embedded in the table top of the MRI scanner. The phased array design allows prolonged volumetric heating of larger volumes of tissue to a homogeneous temperature using MR thermometry as feedback [81]. The above example shows 30 min of *in vivo* hyperthermia treatment in rabbit thigh muscle.
Image courtesy of Steffie Peters.

3.1. Temperature-sensitive liposomes

In pioneering work, Yatvin and Weinstein explored TSLs containing neomycin or methotrexate for targeted delivery (Fig. 4) [20,21]. These TSLs were based on dipalmitoylphosphatidylcholine (DPPC) with a gel–liquid to crystalline (melting) phase transition temperature (T_m) of 41.5 °C. At T_m, the permeability of the lipid bilayer increases significantly due to grain boundaries between gel- and liquid-crystalline

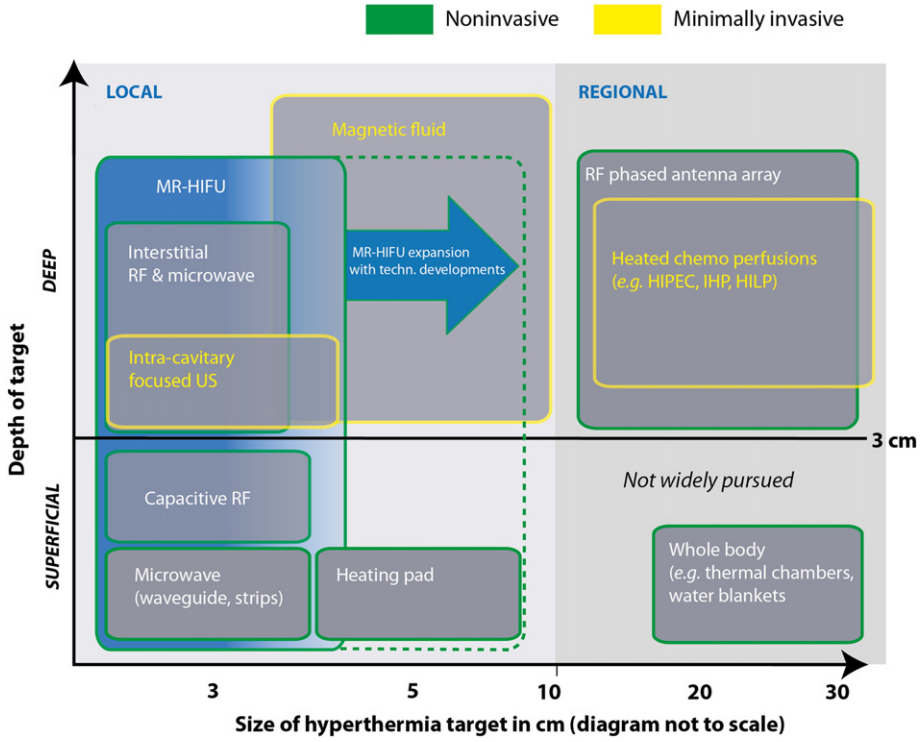

Fig. 3. The hyperthermia technology landscape. MR-HIFU has the potential for moving towards larger volume hyperthermia with technological developments.

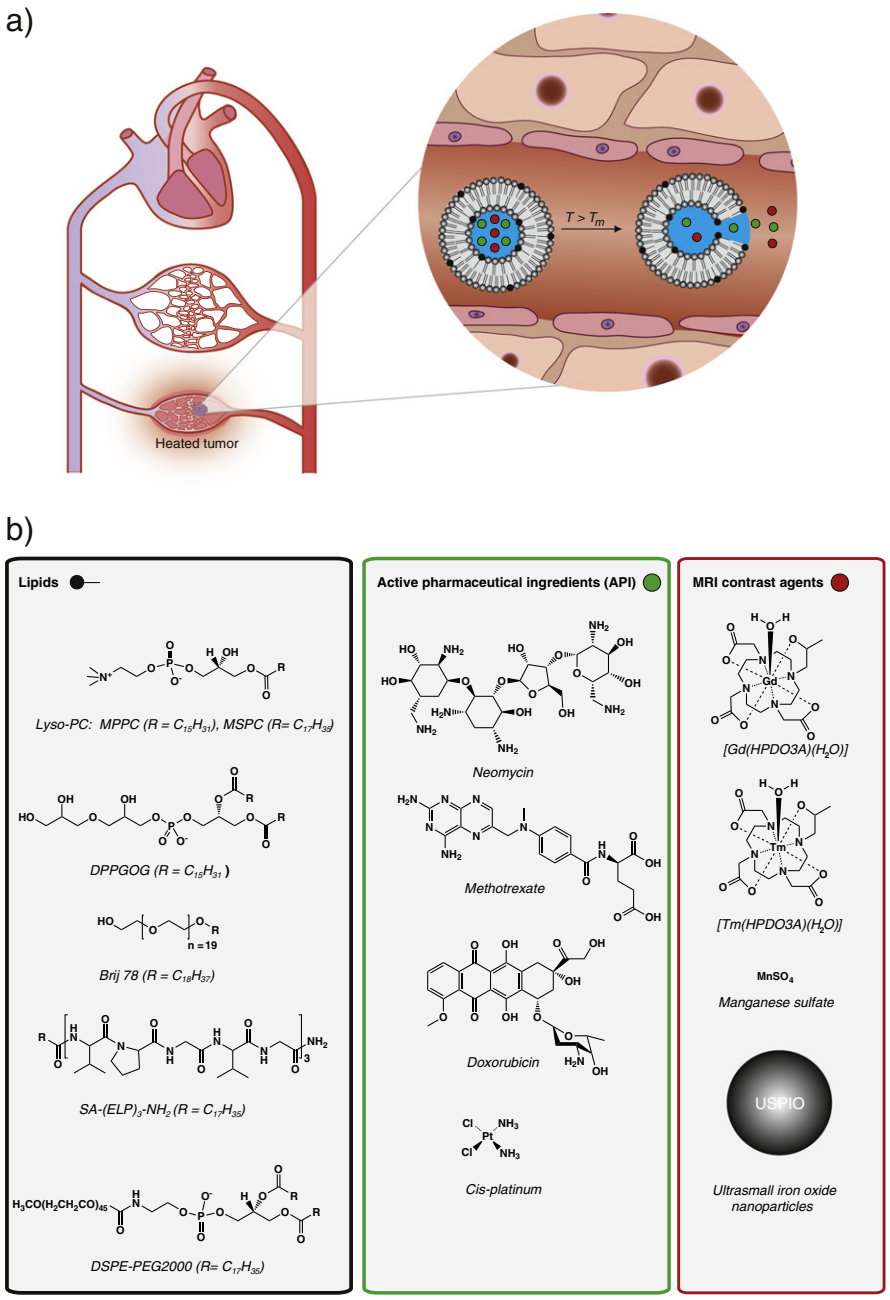

Fig. 4. (a) The concept of intravascular temperature-induced drug delivery under image guidance. Temperature-sensitive liposomes co-encapsulating drugs and MRI contrast agents release their inner content at the melting phase transition temperature of the lipid bilayer. (b) Lipids, active pharmaceutical ingredients and MRI contrast agents that have been incorporated in the lipid bilayer or (co)-encapsulated in the lumen of the TSL, respectively.

domains, thereby facilitating the release of hydrophilic solutes from the liposomal interior. The phase transition temperature of the lipid bilayer has been increased by the incorporation of distearoylphosphatidylcholine (DSPC, $T_m = 55$ °C) in the lipid bilayer [90]. Shortcomings of TSLs composed of DPPC:DSPC (3:1 molar ratio) are the rather slow (10ths of minutes) and incomplete drug release (approx. 30–60%) at elevated temperatures, depending on the exact formulation, parent drug and medium.

An innovative class of temperature-sensitive liposomes that release the entrapped drug in manner of seconds at hyperthermic conditions has been reported by Needham and coworkers [91–96]. In their seminal work, a low temperature-sensitive liposomal (LTSL) formulation based on a lysolipid (*i.e.* monopalmitoylphosphatidylcholine (MPPC) $T_m =$ 34 °C), a PEGylated lipid (*i.e.* DSPE-PEG2000) and DPPC was engineered [92,95,96]. The quick and quantitative drug release from the interior of these LTSLs at elevated temperatures was ascribed to the formation of pore-like defects in the liposomal bilayer that were stabilized by micelle forming phospholipids, such as lysolipids and also PEGylated phospholipids [97,98]. Thanks to their shape factor, *i.e.* a relatively large hydrophilic head group compared to the mono-acyl chain, lysolipids and PEGylated lipids can populate highly curved interfaces and thus stabilize pores along the grain boundaries that form in the bilayer. Moreover, bilayer-incorporated PEGylated-phospholipids provide a steric barrier that slows down opsonization and prolongs blood circulation times, the so-called "stealth effect" [99]. In next generation LTSL formulations, MPPC was replaced with monostearylphosphatidylcholine (MSPC), which shifts the melting phase transition temperature 1° up [22,100]. Recently, material and formulation aspects of LTSLs have been comprehensively reviewed [94]. The notion that amphiphilic molecules with a shape factor suitable to stabilize highly curved pores are essential for

TSLs triggered the design of alternative temperature-sensitive liposomal systems [101–104]. For instance, Brij78-based TSLs (Fig. 4) with acceptable drug retention at body temperature and near-complete drug release within minutes at 42 °C have been reported by Tagami et al. [103]. Recently, Park et al. introduced a novel class of TSLs containing an amphiphilic elastin-like polypeptide (ELP) conjugated to stearylic acid (SA-$(ELP)_3$-NH_2, Fig. 4), DPPC, DSPE-PEG2000, and cholesterol [104]. The temperature sensitivity of this TSL formulation originates from a conformational change of the elastin-based lipid from a random coil to a β-turn upon heating rendering the polypeptide head group more hydrophobic as well as inducing a change in the shape factor [104,105]. Not only does the lipid bilayer determines the release properties and stability of TSLs but also the nature and molecular properties of the encapsulated parent drug and the way retention of the latter is achieved in the interior of the liposome. For example, Kheirolomoom et al. used a copper(II) gluconate solution as an interior buffer to load doxorubicin into a LTSL system similar to the approach of employing a manganese(II)-sulfate buffer for loading [106,107]. The formed copper(II)–doxorubicin complex decreases unintended leakage of doxorubicin and improves blood stability at body temperature compared to LTSL systems using an ammoniasulfate buffer for loading [108].

Another novel TSL formulation has been introduced by Lindner et al. based on 1,2-dipalmitoyl-*sn*-glycero-3-phosphoglyceroglycerol (DPPGOG, Fig. 4), DPPC, and DSPC [101]. Interestingly, this TSL displays a prolonged blood circulation time, stable retention of doxorubicin at body temperature, and fast drug release at hyperthermic temperatures though any PEGylated lipids or lysolipids were omitted [102].

3.2. Image-able temperature-sensitive liposomes

The concept of liposomes containing paramagnetic structures, such as manganese (Mn^{2+}) or gadolinium (Gd^{3+}) chelates, has been explored in the context of liposomal contrast agents for (molecular) MR imaging [109–115]. Encapsulation of the MRI contrast agent (CA) within the liposomal carrier decreases the apparent longitudinal relaxivity (r_1) of the native CA due to a limited transmembrane water exchange rate [116,117]. This effect has been studied to probe the water permeability of the lipid bilayer as a function of lipid composition and temperature [118]. The release of the encapsulated MRI contrast agents from the lumen of the liposome restores the longitudinal relaxivity (r_1) of the native MRI CA, which has been investigated with MR imaging for possible application in image-guided drug delivery though no drugs were yet included in these formulations [119–124]. Viglianti et al. were the first to develop a MR image-able TSLs co-encapsulating the drug doxorubicin and paramagnetic Mn^{2+} that are released simultaneously upon heating [107]. In their milestone publication, the concept of MR image-guided drug delivery using TSLs was demonstrated in a preclinical study [107,125]. Subsequently, de Smet et al. reported on paramagnetic TSLs containing a clinically approved MRI CAs, *i.e.* [Gd(HPDO3A)(H_2O)] (Fig. 4), that was co-encapsulated with doxorubicin [126]. In recent years, more TSL formulations of doxorubicin with clinically approved Gd-chelates have been studied for local drug delivery under MR image guidance [86,127,128]. An innovative concept for image-guided drug delivery was proposed by Langereis et al. In their work, chemical exchange saturation transfer (CEST) and ^{19}F-MR imaging have been exploited to probe the release of hydrophilic structures from the lumen of TSLs [129]. To this end, [Tm(HPDO3A)(H_2O)], a thulium-based chemical shift agent, and ammonium hexafluorophosphate (NH_4PF_6) were compartmentalized in the interior of a TSL (Fig. 4), which allowed visualization of the intact liposomes based on the CEST effect. Upon release of the chemical shift the CEST MR signal is lost, whereas the ^{19}F MR signal is restored. Therefore, this approach allows in principle the MR visualization of the liposomal carrier and MR image guidance of drug release. Recently, Lorenzato et al. designed temperature-sensitive magnetoliposomes as a tool for MR image-guided drug delivery [130]. The MR contrast enhancement of the liposomes encapsulating ultrasmall superparamagnetic iron oxide nanoparticles (USPIO, Fig. 4) changed significantly at the melting phase transition temperature, allowing tracking of the liposomes before release and imaging of the release process itself (Fig. 5). Table 1 gives an overview of the temperature-sensitive liposomal formulations that have been explored for image-guided drug delivery.

4. Preclinical studies

The *in vivo* applications of liposomal systems for image-guided drug delivery have been recently reviewed in depth [134,135]. Therefore, we would like to summarize the main concepts and contributions for temperature-induced drug delivery using HIFU as heating device with special attention to studies performed under MR-image guidance.

4.1. Image-guided drug delivery studies

TSLs have been studied for MR image-guided drug delivery in various tumor models with different heating techniques [85,108,125]. In general, most preclinical studies employed doxorubicin as a parent drug and the targeted tumor was heated to mild hyperthermia. For intravascular release, TSLs were injected either before heating or while heating was ongoing. Consequently, a high peak blood concentration of doxorubicin was obtained, providing a steep concentration gradient that drives doxorubicin uptake in the tissue. The milestone study by Viglianti et al. was performed in a rat model bearing a subcutaneous fibrosarcoma (FSA) tumor. The tumor was heated using an interstitial catheter flushed with heated water to trigger local drug release. The observed signal change upon co-release of Mn^{2+} with doxorubicin allowed an MR imaging based quantification of doxorubicin in the heated tissue establishing the concept of dose painting for image-able liposomes in combination with MRI. Taking this concept further, Ponce et al. showed that the antitumor effect scaled with the doxorubicin concentration that was indirectly estimated from MRI [132]. A clear correlation between the intratumoral doxorubicin concentration and the MR contrast change was also found in several studies using the gadolinium-based MRI contrast agents [Gd(HPDO3A)(H_2O)] and $[Gd(DTPA)(H_2O)]^{2-}$ [85,128]. MR-HIFU-mediated drug delivery under MR image guidance using TSLs containing [Gd(HPDO3A)(H_2O)] and doxorubicin was first demonstrated in rats bearing a subcutaneous gliosarcoma tumor [85]. Here, MR-HIFU was used to establish two times 15 min of hyperthermia. The release of [Gd(HPDO3A)(H_2O)] was followed with intermittent mapping of the longitudinal relaxation time (T_1) [83,85]. Similar to the study of Ponce et al., Tagami and coworkers showed that the MR contrast change caused by the release

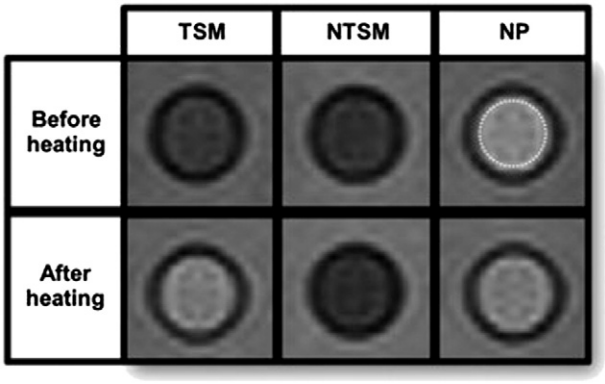

Fig. 5. T_1-weighted gradient echo images (echo time 10 ms) before and after heating to 45 °C using a waterbath for thermosensitive liposomes (TSM), non-thermosensitive liposomes (NTSM) and free iron oxide particles (NP). A clear MRI signal enhancement of 83 ± 4% is shown for TSM.
Reprinted with permission from Wiley [130].

Table 1
Overview of the liposomal formulations used in image-guided temperature-induced drug delivery studies. ADC = apparent diffusion coefficient, P_{ac} = applied acoustic power, PRFS = proton resonance frequency shift thermometry, DOX = doxorubicin, DSPG = distearoylphosphatidylglycerol, $DPPG_2$ = 1,2-dipalmitoyl-*sn*-glycero-3-phosphodiglycerol, HaT = hyperthermia-activated cytotoxic.

Reference	Study	Hyperthermia technology	Temperature monitoring	Type	Liposomal formulation (molar ratio)	Drug	Intraliposomal MRI CA (concentration in lumen)
Fossheim et al. [119]	Phantom	Microwave irradiation	Estimated from MR ADC measurements	TSL	DPPC:DPPG (47.5 and 2.5 mg/mL)	NA	[Gd(DTPA-BMA)(H_2O)] (250 mM)
Frich et al. [131]	*In vivo*	Radiofrequency and laser (Nd-YAG) ablation	Fiber optics	TSL	DSPC:DSPG (90:10 w/w)	NA	[Gd(DTPA-BMA)(H_2O)]
McDannold et al. [121]	*In vivo*	MR-HIFU system (1.7 MHz)	PRFS thermometry	TSL	DSPC:DSPG (90:10 w/w)	NA	[Gd(DTPA-BMA)(H_2O)] (250 mM)
Ponce et al. [132], Viglianti et al. [125]	*In vivo*	Heated water flow through a catheter placed through the center of the tumor	ECG electrodes and rectal temperature probe	LTSL	DPPC:MSPC:DSPE-PEG2000 (90:10:4)	DOX	$MnSO_4$ (300 mM)
Peller et al. [123], Wang et al. [122]	*In vivo*	Water bath			DPPC:DSPC:DPPGOG (50:20:30)	NA	[Gd(DTPA-BMA)(H_2O)] (250 mM)
Langereis et al. [129]	Phantom	Water bath		LTSL	MPPC:DPPC:DPPE-PEG2000 (10:90:4)	NA	[Tm(HPDO3A)(H_2O)] (65 mM) and NH4PF6 (50 mM)
De Smet et al. [85]	*In vivo*	MR-HIFU clinical system with dedicated animal setup (P_{ac} = 8 W, 1.4 MHz)	PRFS thermometry	TSL	DPPC:HSPC:Chol:DPPE-PEG2000 (50:25:15:3)	DOX	[Gd(HPDO3A)(H_2O)] (250 mM)
Negussie et al. [127]	*In vivo*	MR-HIFU clinical system (1.2 MHz)	PRFS thermometry	LTSL	DPPC:MSPC:DSPE-PEG2000 (85.3:9.7:5.0)	DOX	[Gd(HPDO3A)(H_2O)] (300 mM)
Tagami et al. [128]	*In vivo*	Water bath	ECG electrodes and rectal temperature probe	HaT	DPPC:Brij78 (96:4)	DOX	$[Gd(DTPA)(H_2O)]^{2-}$ (100 mM)
Lorenzato et al. [133]	Phantom	MR-HIFU system (1.5 MHz)	PRFS thermometry and fiber optics	TSL	DPPC:HSPC:Chol:DSPE-PEG2000 (100:33:27:7)	NA	USPIO
Hossann et al. [124]	*In vitro*	Water bath		TSL	DPPC:DSPC:$DPPG_2$ (50:20:30)	NA	$[Gd(DTPA)(H_2O)]^{2-}$ [Gd(HPDO3A)(H_2O)] [Gd(BTDO3A)(H_2O)] $[Gd(DOTA)(H_2O)]^{-}$ $[Gd(BOPTA)(H_2O)]^{2-}$ [Gd(DTPA-BMA)(H_2O)] iso-osmolar to physiological solutions

of Gd-CA can be used to quantify the doxorubicin concentration in the tumor and furthermore allows to predict the tumor response in mice [128]. Though these Gd-based MR contrast agents are less retained in the tumor tissue upon release than Mn^{2+}, and have very different pharmacokinetics than doxorubicin, both studies show a clear correlation between the T_1-contrast change before and after hyperthermia, and the tumor averaged doxorubicin concentration. However, due to the different pharmacokinetic properties of doxorubicin and these Gd-CAs, the correlation between the T_1 contrast change and doxorubicin concentrations is different, most likely due to tumor specific characteristics, such as perfusion, microvessel permeability (*i.e.* k_{trans}), or the presence of a necrotic core.

Wood et al. co-encapsulated [Gd(HPDO3A)(H_2O)] with doxorubicin in a LTSL and used this formulation in preclinical rabbit studies with MR-HIFU heating [86,87,127]. These studies demonstrated the basic concept of image-guided drug delivery, where T_1-weighted MR image contrast enhancement allows assessment of the drug delivery process during the intervention. Unfortunately, no direct correlation between T_1-contrast change and doxorubicin concentrations in the tumor was shown, though the study clearly demonstrated the potential of temperature-induced drug delivery to achieve high drug concentrations in hyperthermia treated tissue. T_1-maps revealed strong intratumoral inhomogeneities and intertumoral variations, providing an argument that image-guided drug delivery may provide a tool for personalized tumor therapy [85]. Though the above image-guided drug delivery studies differ in TSL formulation, heating method and protocol, contrast agent, and tumor model, the similar findings suggest that the basic concept is suitable for clinical translation.

An interesting study was recently reported by Kheirolomoom et al. on temperature-induced drug delivery by ultrasound heating (not performed under MR image guidance) [108]. This study was performed with an innovative formulation of doxorubicin in a LTSL, where copper (Cu^{2+}) was used for doxorubicin loading (Cu-dox-LTSL). The latter formulation performed superior compared to a classical LTSL formulation with respect to drug leakage at body temperature, while maintaining rapid drug release at elevated temperatures. A survival study was performed with this formulation in mice bearing a subcutaneous NDL tumor. While most preclinical studies so far performed one single treatment, this study used a more complex treatment scheme, including 5 min of pre-heating prior administration of the drug, and two times 20 min hyperthermia mediated drug delivery treatments per week for 4 weeks (Table 2). The survival study (Fig. 6) showed complete remission in the treatment group, compared to the control arms that received hyperthermia alone or Cu-dox-LTSL without heating.

The above study demonstrates the enormous potential of local drug delivery for local tumor control and motivates to further investigate protocols for future clinical application in a preclinical setting. The status of all HIFU studies with details on protocols, temperature monitoring and achieved drug concentrations in the targeted tissue is summarized in Table 2.

4.2. Interference of MR-contrast agents with MR temperature mapping

A potential complication associated with the use of paramagnetic liposomes for MR image-guided temperature-induced drug delivery is the effect of the paramagnetic structures or chemical shift agents on MR-based thermometry used for temperature feedback on the HIFU treatment. Hijnen et al. studied this effect *in vitro* and *in vivo*, showing that both the absolute presence and the change in the concentration of Gd-ions affected the PRFS-based temperature maps (Fig. 7). The presence of paramagnetic Gd-based MRI contrast agents in the target tissue induced temperature errors ranging between −4 °C and +3 °C during MR-HIFU ablation experiments, where Gd-enhanced scans are acquired during the planning phase of the treatment [136].

Based on these results, the consequences for image-guided drug delivery using image-able liposomes was re-analyzed for the studies performed by de Smet et al. [137]. Here, the change in the concentration of Gd-ions is minimal as long as the ions are encapsulated by the liposomal carrier and injected prior to the onset of MR based thermometry thanks to the long blood circulation time of the paramagnetic liposomes compared to the heating duration. However, upon heating, the Gd-ions are released into the blood and surrounding tissue, resulting in different spatial distributions and concentrations of paramagnetic ions in the heated area. The Gd-concentration in the tumor after 15 min of hyperthermia treatment can be estimated from the change in the longitudinal relaxation rate (R_1) before and after heating ($\Delta R_1 = 0.15 \pm 0.10\ s^{-1}$ (rhabdomyosarcoma) [137], $\Delta R_1 = r_1 \cdot \Delta[Gd]$, $r_1 = 3.7\ L\ mmol^{-1}\ s^{-1}$ [138], $\Delta[Gd] = 0.04 \pm 0.03$ mM). Assuming a spherical tumor, such change in Gd-concentrations would result in temperature errors around -0.9 ± 0.6 °C on the border zone of the rhabdomyosarcoma tumors. Furthermore, the presence of Gd-ions changes the temperature dependency of the screening constant used to calculate temperature changes from the measured phase changes in PRFS thermometry. At the typical Gd-concentrations obtained during image-guided drug delivery (max. 0.3 mM), the error in PRFS thermometry due to this effect was estimated to be below 1%. Furthermore, no difference in susceptibility was observed when the contrast agents were released from the temperature-sensitive liposomes [136]. It should be noted, however, that the Gd-concentration that is reached during the drug delivery varies per tumor type and depends on the vessel permeability and the heating protocol. Thus, above considerations may be different for other studies using image-able liposomes while using MR thermometry. Awareness should be generated that the use of gadolinium and other MRI contrast agents interferes with PRFS thermometry and may lead to false thermal doses. Although complicated, correction methods for the presence of paramagnetic ions in tissues during PRFS thermometry are urgently needed.

4.3. Intratumoral distribution of liposomes

Hyperthermia increases tissue perfusion and the permeability of blood vessels, thereby promoting liposome extravasation into the targeted tissue. The effect of hyperthermia on TSL extravasation from the tumor vasculature using a window chamber model has been studied first by Kong et al. [51]. More recently, Li et al. used a window chamber model to investigate the hyperthermic conditions required to improve the extravasation and interstitial penetration of liposomes in four different murine tumor models (B16 melanoma, BFS-1 sarcoma, LLC carcinoma, BLM melanoma) [139]. Without hyperthermia, no extravasation of liposomes was observed for the first 2 h after injection. Twenty to 30 min of hyperthermia at 41 °C were required to initiate the extravasation of liposomes with a diameter of 85 nm. The liposome intensity in the extracellular space kept increasing when the heating was prolonged to 1 h at 41 °C in all tumor models but leveled off at times beyond 4–8 h. The penetration depth of the liposomes into the extracellular space was dependent on the specific tumor model (10 μm–27.5 μm). After hyperthermia, the tumor vasculature remained permeable for 8 h. The latter effect is important as it may contribute to increased drug levels *via* accumulation of yet drug filled TSLs. To that aim, de Smet et al. designed radiolabeled TSLs that allowed following the biodistribution and tumor uptake of the liposomes in gliosarcoma bearing rats using SPECT nuclear imaging 48 h after hyperthermia. Fig. 8 shows the biodistribution of the TSLs, with high uptake in the clearance organs liver and spleen. MR-HIFU-induced hyperthermia increased the TSL uptake in this tumor model by a factor of 4.4, while the doxorubicin concentration increased by a factor of 7.9 (48 h after HT). The SPECT scans revealed a high intratumoral inhomogeneity and intertumoral variations, consistent with earlier results [85].

The same group studied the intratumoral distribution of TSLs after HIFU-mediated hyperthermia in more detail using autoradiography in a rat rhabdomyosarcoma tumors [137]. At 48 h, when the liposomes were almost completely cleared from the blood stream, the autoradiography pictures mainly reflect the extravasated liposomes (Fig. 9). On the tumor level, areas were observed with low and particularly high TSL uptake. The tumor areas where a high liposomal concentration was observed on autoradiography, was largely congruent to the areas of high doxorubicin tissue concentrations and nonviable tissue on histology. This indicated that the doxorubicin concentrations that reached these areas after a single treatment were high enough to induce cell death, while other areas did not yet receive a sufficient dose. Repeated treatments would be required to treat also the less perfused tumor parts. Another attractive option would be to use the versatility of the HIFU technology by thermally ablating the less perfused tumor parts.

The liposomal biodistribution data suggests that HIFU-mediated hyperthermia facilitates liposomal extravasation and accumulation over a considerable time span subsequent to the hyperthermia treatment. This advocates the development of more stable TSL formulation as the longer-term accumulation of yet drug filled liposomes may add to the intravascular release of the drug during the hyperthermia treatment.

4.4. Intratumoral distribution of doxorubicin

Several studies investigated the drug distribution across the tumor tissue after temperature-induced drug delivery. In an elegant study using a window chamber model, Manzoor et al. visualized with confocal microscopy the intravascular release of doxorubicin from a TSL [141]. Fig. 10a shows the intravascular influx of TSLs, the subsequent release of doxorubicin upon heating, and the extravasation of doxorubicin into the surrounding tissue. A quantitative analysis (Fig. 10b) shows that temperature-induced drug delivery provides higher doxorubicin concentrations at farther distances from the blood vessels compared to non-temperature-sensitive liposomes filled with doxorubicin, or free doxorubicin.

Staruch et al. performed a drug delivery study in rabbits bearing an intramuscular VX2 tumor using HIFU for local heating. Temperatures were assessed *in vivo* using PRFS MR thermometry to provide a feedback to the HIFU transducer. In this experiment, a LTSL formulation (ThermoDox®, Celsion Corporation) was infused within the first 5 min of a total heating period of 20 min. Analysis of the doxorubicin concentration in heated and unheated tumor tissue showed a 26 fold increase of drug concentration with heating reaching up to 76.3 ± 27.9 μg/g doxorubicin in the heated tumor (Table 2). Fig. 11 shows the histological analysis of the tumor tissue, nicely demonstrating the co-localization of doxorubin with the cell nuclei in the heated tissue, and the homogeneous uptake in cells distant to blood vessels. The latter was confirmed in rhabdomyosarcoma rat tumors by de Smet and Hijnen et al. [137].

5. Protocol considerations for temperature-induced drug delivery

Basically all studies on temperature-induced drug delivery applied heating of the target tissue right after or simultaneous with the injection of TSLs, leading to intravascular release of doxorubicin. Instead of the intravascular release strategy, an extravascular (sometimes referred to as interstitial) release protocol could be used [143]. The most suitable strategy for a particular application depends on the pharmacokinetic properties of the parent drug, the properties of the TSL, *i.e.* circulation time, leakiness and release kinetics, as well as the properties of the targeted tumor, such as permeability of the blood vessels, presence of EPR effect, and perfusion. For the intravascular release strategy, the amount of drug delivered to the target tumor scales to a first approximation with the hyperthermia heating duration, the plasma concentration of TSLs, the drug-payload per liposome, and the blood perfusion of the target tissue [144,145]. Ponce et al. used the MR dose-painting concept to investigate the effect of different TSL injection times with respect to hyperthermia on the temporal and spatial patterns of drug delivery

Table 2
Overview of tissue concentration of doxorubicin (DOX) in temperature-induced drug delivery studies using HIFU. FUS = focused ultrasound, US = ultrasound, P_{ac} = applied acoustic power, prf = pulse repetition frequency, PNP = peak negative pressure, TAP = total acoustic power. Data are expressed as mean ± SD.

Reference	Animal/tumor model or tissue	HIFU	Hyperthermia protocol	Liposome injection	Liposomal formulation	DOX dose (mg/kg)	[DOX] (μg/g tissue)	
							+HIFU	−HIFU
Dromi et al. [155]	Mice/murine mammary adeno-carcinoma	Pulsed HIFU (I_{SATA} = 1300 W/cm^2, 120 pulses, prf 1 Hz, duty cycle 10%)	15–20 min, temperature elevation 4–5 °C	0 or 24 h prior heating	ThermoDox®	2.0	Ca. 3.5 (tumor)	Ca. 1.3 (tumor)
Patel et al. [156]	Mice/SCC7 murine squamous cell carcinoma	Split focus transducer (TAP 20–80 W, 1 MHz duty cycle 10%)	2 min, temperature elevation 3–5 °C	Immediately prior heating	ThermoDox®	5.0	1.7 ± 0.4 (muscle)	0.7 ± 0.1 (muscle)
De Smet et al. [85]	Rat/9L gliosarcoma	MR-HIFU clinical system with dedicated animal setup (P_{ac} = 8 W, 1.4 MHz)	2 × 15 min at 41–42 °C	Upon reaching 42 °C	[Gd(HPDO3A)(H_2O)] & DOX-loaded TSL	5.0	7.4 ± 6.7 (tumor)	1.5 ± 0.6 (tumor)
Negussie et al. [127]	Rabbit/VX2	MR-HIFU clinical system (f_{ac} = 1.2 MHz)	4 × 10 min at 40–42 °C	10 min prior heating	[Gd(HPDO3A)(H_2O)] & DOX-loaded LTSL	5.0	NA	NA
Staruch et al. [147]	Rabbit/muscle	Mechanical scanning (P_{ac} = 16 W, 2.8 MHz), MR guidance	20–30 min at 43.2 ± 0.3 °C	During 8 min upon reaching 43 °C	ThermoDox®	2.5	8.3 ± 6.9 (muscle)	0.5 ± 0.2 (muscle)
Ranjan et al. [88]	Rabbit/VX2	MR-HIFU clinical system	3 × 10 min at 40.5 ± 0.1 °C	During 3 min prior heating	ThermoDox®	5.0	30 ± 9 (tumor)	8.8 ± 1.4 (tumor)
Staruch et al. [157]	Rabbit/ bone marrow/ muscle	Mechanical scanning (P_{ac} = 16 W, 2.8 MHz), MR guidance	20 min at 43 °C	During 8 min upon reaching 43 °C	ThermoDox®	2.5	32 ± 7.4 (muscle) 43 ± 14 (bone marrow)	2.0 ± 0.9 (muscle) 4.3 ± 0.6 (bone marrow)
Partanen et al. [87]	Rabbit/VX2	MR-HIFU clinical system (P_{ac} = 20 W, 1.2 MHz)	30 min total at 40.6 ± 1.0 °C	Prior heating	ThermoDox®	5.0	Ca. 60 (n = 1, tumor sections)	Ca. 15 (n = 1, tumor sections)
Staruch et al. [142]	Rabbit/VX2	Mechanical scanning (P_{ac} = 16 W, 2.8 MHz), MR guidance	20 min at 43 °C	During 8 min upon reaching 42 °C	ThermoDox®	2.5	76 ± 28 (tumor)	3.4 ± 1.8 (tumor)
Gasselhuber et al. [150]	Rabbit/VX2	MR-HIFU clinical system (P_{ac} = 25 W, 1.2 MHz)	3 × 10 min at 41.7 ± 1.1 °C	Prior heating	ThermoDox®	5.0	Ca. 20–30[a] (n = 1)	Ca. 5[a] (n = 1)
De Smet et al. [137]	Rat/ rhabdomyosarcoma	MR-HIFU clinical system with dedicated animal setup (P_{ac} = 10 W, 1.4 MHz)	2 × 15 min at 41 ± 2 °C	Immediately prior heating	[Gd(HPDO3A)(H_2O)] & DOX-loaded ^{111}In-labeled TSL	5.0	Histology	
De Smet et al. [137,140]	Rat/9L gliosarcoma	MR-HIFU clinical system with dedicated animal setup (P_{ac} = 8 W, 1.4 MHz)	2 × 15 min, temperature elevation 4–5 °C	Immediately prior heating	[Gd(HPDO3A)(H_2O)] & DOX-loaded ^{111}In-labeled TSL	5.0	Ca. 10 ± 9.9 (after 48 h)	Ca. 1.3 ± 0.6 (after 48 h)
Kheirolomoom et al. [108]	Mice/NDL	Linear FUS array/US guidance (100-cycle bursts, 1.5 MHz, PNP = 1.1 MPa, PRF = 0.1 to 5 kHz), thermocouples	42 °C for 5 min before and 20 min after LTSL injection	After 5 min pre-heating at 42 °C	Cu-DOX-LTSL (copper as loading agent, LTSL based on MPPC)	6 mg/kg delivered twice per week for 4 weeks	NA, Survival study: complete remission for HIFU treated group	

[a] Line profile of doxorubicin measured with microscopy.

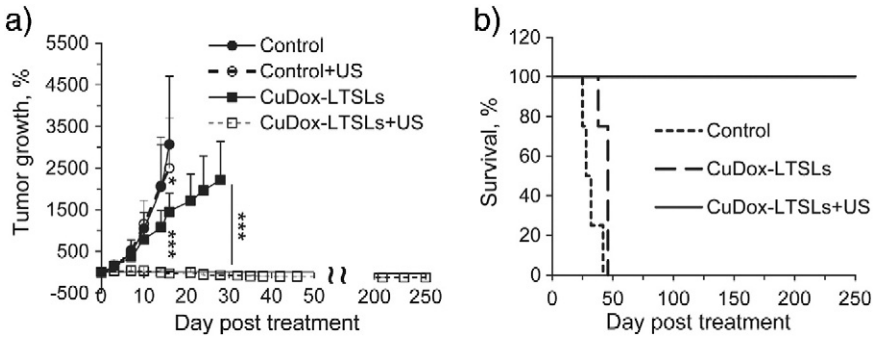

Fig. 6. *In vivo* treatment efficiency including ultrasound (US), and Cu-dox-LTSLs with and without US in NDL tumor mice. (a) Tumor growth as a function of days post treatment. Initial tumor diameter was 4 mm. Each mouse was injected intravenously with either saline or liposomal doxorubicin (6 mg doxorubicin/kg body weight equivalent to 33 mg/m^2) and compared to control animals that received intravenous injection of saline. For treatment with ultrasound-mediated hyperthermia, one tumor per animal was insonified at 42 °C for 5 min prior to and 20 min post-injection. (b) Kaplan–Meier survival plot. Statistical analyses were performed using one-way ANOVA followed by the Tukey post hoc test. *$p < 0.05$ and ***$p < 0.001$. Reprinted with permission from Elsevier [108].

[132]. They showed that the drug delivery pattern varied upon the injection time of the TSL, with injection before hyperthermia treatment yielding drug delivery in the center of the tumor, while TSL injection during hyperthermia resulted in a peripheral drug distribution. The latter strategy was most effective in delaying the tumor growth [132]. Thus, TSL injection should be performed as soon as the target tissue reached hyperthermic temperatures, or at least, heating should start immediately after TSL injection or infusion.

Furthermore, the intravascular release approach requires the TSLs to rapidly release their payload at mild hyperthermic temperatures as drug release and subsequent tissue uptake needs to compete against downstream washout. The latter scales with tumor perfusion and thus the tumor transit time and may therefore vary for each tumor (>20 s for a 2 cm diameter tumor) [22]. The optimal release time constant for TSLs for intravascular drug delivery was calculated to be below 3 s (time release constant was defined as the time after which 63% of the content was released) [146]. The major benefit of the intravascular release strategy is that high intravascular drug concentrations are created that drive drug uptake by cells and increase drug penetration into the tumor tissue (>50 μm away from the blood vessel wall) reaching also tumor cells located further away from blood vessels [86,137,147].

For the extravascular release strategy, waiting time (*e.g.* 24 h) is built into the treatment protocol after systemic injection of the TSLs to allow time for the liposomes to extravasate in the tumor tissue. Subsequently,

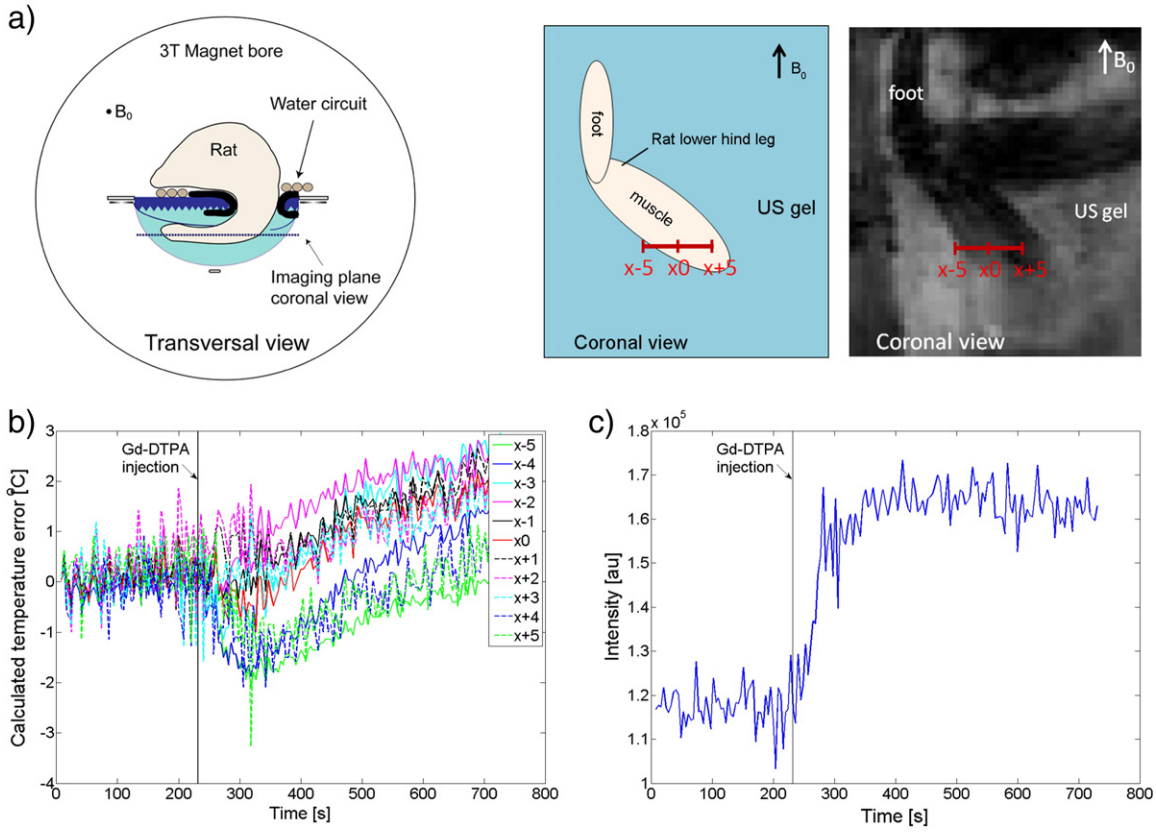

Fig. 7. (a) Schematic drawings of the animal orientation in transversal and coronal directions, and a magnitude image of the rat hind leg as obtained with the PRFS thermometry sequence (coronal view). The red scale bar indicates the voxel locations in plot (b). (b) The perceived temperature baseline error over time *in vivo* over a horizontal line profile in the rat muscle. (c) PRFS voxel signal intensity data obtained at x0 indicating the inflow of $[Gd(DTPA)(H_2O)]^{2-}$ into the rat hind leg muscle [136].

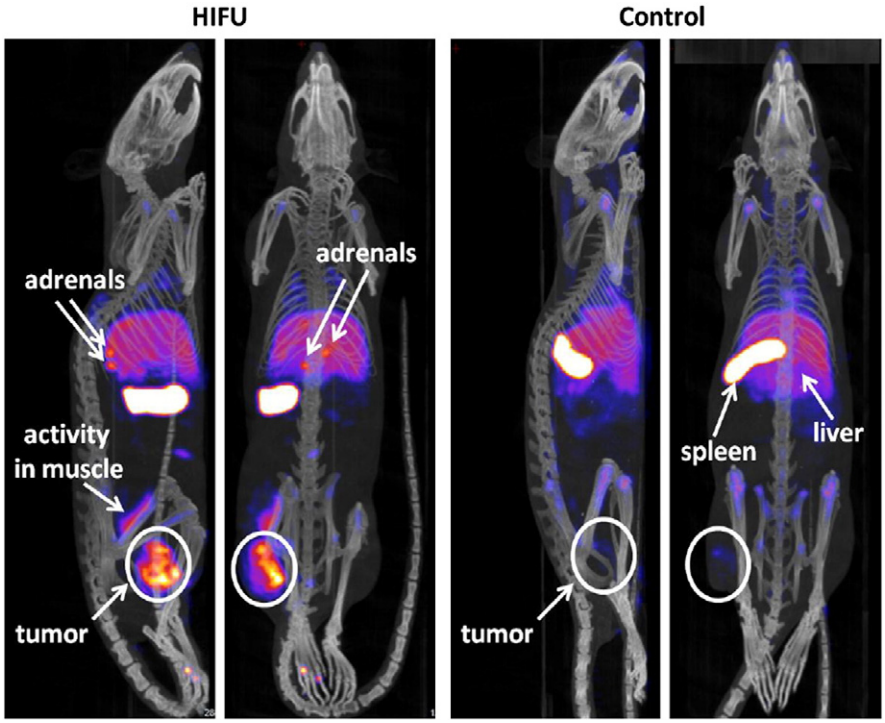

Fig. 8. SPECT/CT images of gliosarcoma tumor bearing rats 48 h after TSL injection. HIFU-mediated hyperthermia of the tumor in combination with radiolabeled TSLs (left), and a control experiment with radiolabeled TSLs without HIFU treatment (right).
Reprinted with permission from Elsevier [140].

the target tissue is heated to release the drug and render it bioavailable. Due to the time required for extravasation and accumulation of the liposomes in the tumor, TSLs need to stably encapsulate the drug at body temperature but may compromise on the release rate at elevated temperatures. The amount of liposomes that accumulates in the tumor tissue scales with the EPR effect of the tumor, which is known to be very heterogeneous and differs largely between tumor models and species, and may even be absent in many human tumors [19]. The extravascular release approach may be particularly beneficial for hydrophilic drugs that suffer from a rapid wash-out and would therefore not be taken up and retained in the tumor sufficiently upon intravascular release. Next to the heterogeneous vessel permeability, the main limitation of

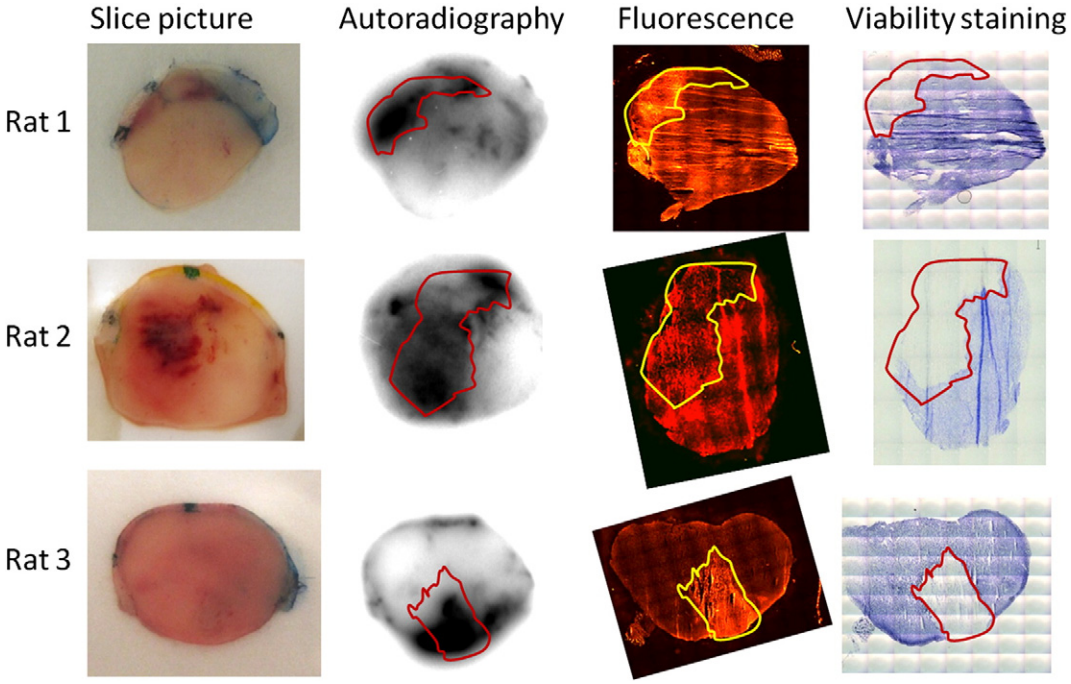

Fig. 9. Pictures, autoradiography, fluorescence signal intensity in the doxorubicin channel, and viability NADH staining of all tumors dissected 48 h after hyperthermia treatment. The red/yellow contour indicates the necrotic area as determined based on the NADH staining, which is overlayed on the autoradiographic image and on the fluorescence image taken from the same histology slice.
Adapted and reprinted with permission from Lippincott Williams & Wilkins [137].

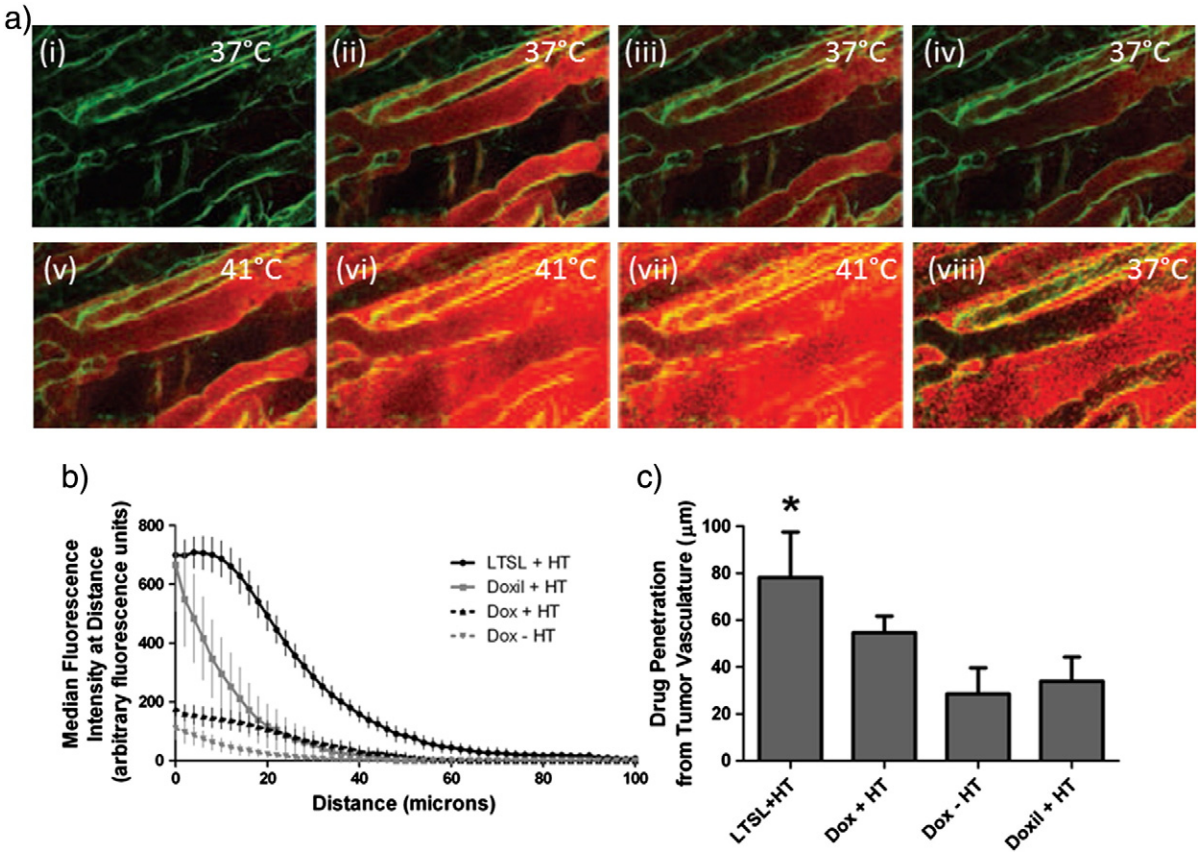

Fig. 10. (a) A time series of intravascular release of doxorubicin from TSL in the eNOS-GFP mouse model is shown. The green GFP signal is restricted to the endothelial cell layer. (i) Background vessels before injection. (ii) Immediately after injection (bolus phase, 0.5 min) of doxorubicin (red) containing TSL at 37 °C. (iii) and (iv) 2 to 5 min post injection at 37 °C. (v), (vi), and (vii) 1, 5 and 15 min after onset of heat treatment at 41 °C. (viii) 10 min after stopping heat, most unbound free doxorubicin is washed out of the bloodstream and doxorubicin-stained nuclei remain fluorescent. Scale bar, 100 mm. (b) Quantitative assessment of drug penetration from blood vessels in a flank tumor model. Drug levels as median fluorescence intensity are shown at distances out to 100 µm from the nearest blood vessel. Hyperthermia combined with LTSL, Doxil®, and free doxorubicin are compared. (c) The maximum drug penetration from tumor vasculature *versus* treatment group. Data are expressed as medians (b) and means (c) with SD.
Reprinted with permission of American Association for Cancer Research [141].

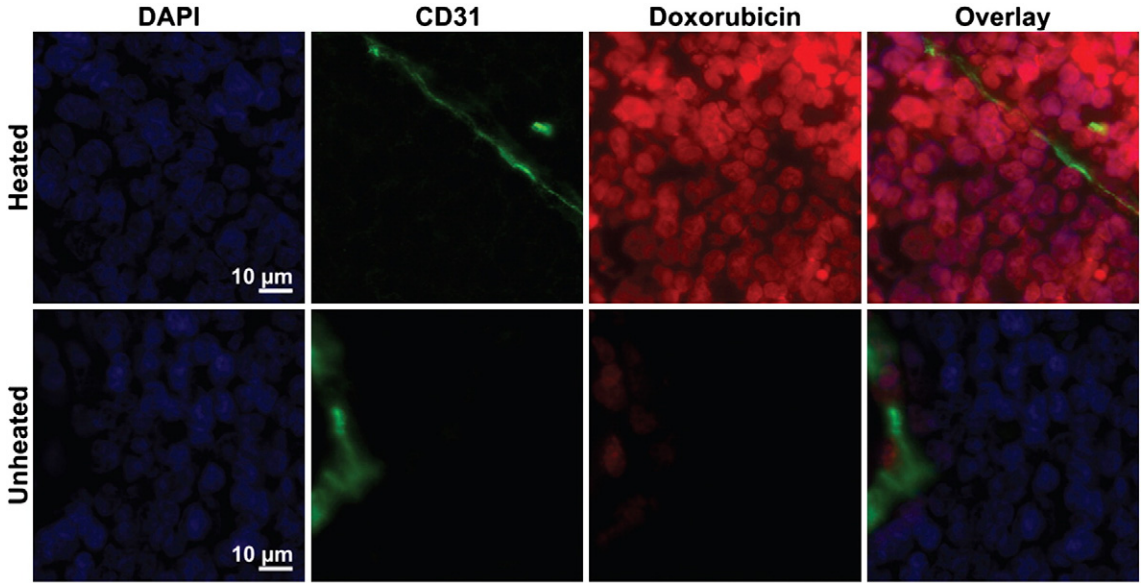

Fig. 11. Accumulation of doxorubicin in heated and unheated rabbit VX2 tumors, following administration of thermo-sensitive liposomal doxorubicin. Doxorubicin fluorescence (red), DAPI-stained cell nuclei (blue), and CD31-stained blood vessels (green) are shown.
Reprint with permission from Informa UK Ltd [142].

the extravascular approach is the small penetration depth of liposomes into the interstitial space, resulting in perivascular 'hot spots' of extravasated liposomes (within 30 μm distance from the leaky vessel wall) [148]. In case extravasated TSLs are taken up by cells prior to hyperthermia-induced drug release, the drug will be release intracellularly limiting drug coverage of the entire tumor [149].

Recently, Gasselhuber et al. compared the intra- and extravascular release strategy for TSLs loaded with doxorubicin using mathematical modeling [146]. In their model, the intravascular release strategy comprising TSLs with a high doxorubicin release rate of 0.3 s^{-1} afforded approximately 6 times higher intracellular tumor concentrations of doxorubicin than the extravascular release strategy using "slow" drug release TSLs (100.6 μg/g intravascular release *versus* 15.9 μg/g for extravascular release). The lower intracellular tumor tissue concentration upon extravascular release suggested back diffusion of the released doxorubicin into the blood plasma [141,146]. Cellular uptake of the liposomes prior release, however, would reduce back diffusion and was not considered in the model. The model was compared to a drug delivery experiment using MR-HIFU for local heating in combination with a LTSL formulation of doxorubicin. Taking all experimental parameters into account, the calculated tissue concentration of doxorubicin across the heated area compared well to the measured concentration (Fig. 12). An overview of the doxorubicin concentrations in tissue obtained in different preclinical studies is shown in Table 2.

The model of Gasselhuber et al. allows simulation of appropriate treatment protocols for drugs and TSL systems under consideration and should be used in the design of formulations as well as the entire study design. The importance of study design was recently pointed out by the results of the HEAT randomized phase III clinical trial where RF ablation alone was compared to RF ablation in combination with drug delivery from ThermoDox® for the treatment of larger (>3 cm^3) HCC liver tumors [151]. Preclinical studies demonstrated that the administration of liposomal encapsulated doxorubicin prior to RF ablation therapy leads to accumulation of liposomal doxorubicin in a peripheral rim of tumor adjacent to the zone of coagulation, sometimes resulting in an increased coagulation diameter over 48 h after therapy [152,153]. However, early results of the phase III clinical study showed that the trial was not successful when measured by its primary endpoint of showing 33% improvement in progression free survival (80% power, p-value 0.05) [154]. Post-hoc analysis of the data showed that patient selection (single lesion only) and the duration of heating (>45 min) giving enough time for the liposomes to deposit high concentrations of doxorubicin were key factors for successful clinical outcome [154]. As mentioned earlier, the amount of drug delivered directly relates to the heating duration which is rather short in the case of ablation treatment [150]. With MR-HIFU, the device used for the ablation can also be used for heating to hyperthermic temperatures, allowing adaption of the heating protocols to the specific application (*e.g.*, longer duration heating when adjuvant drug delivery is needed).

6. Conclusions and outlook

The concept of temperature-induced drug delivery has been introduced more than 30 years ago. Since then, important steps have been taken in chemistry and engineering developing TSLs and technologies for noninvasive local heating to a level ready for clinical translation. A plethora of preclinical evidence has been generated that temperature-induced drug delivery provides significantly higher drug concentrations in the targeted tumor and increase drug penetration in the tissue, showing the value of this approach. While in the preclinical setting several heating methods exist to maintain local and well-controlled hyperthermia, clinical application would strongly benefit from a technology for controlled hyperthermia under noninvasive temperature guidance. Here, MR-HIFU provides a unique solution for local to regional heating of deep seated tissue to well-defined temperatures.

The clinical application of temperature-induced local drug delivery requires approval of a drug-device combination marrying technology with chemistry. The marriage contract will be a dedicated clinical treatment protocol taking into account all aspects of the TSL, the technology, and aspects specific to the target disease. However, before this couple walks down the aisle, several challenges have to be tackled:

- *Hyperthermia technology*: The hyperthermia technology should offer high spatial control over the heated areas, where volume and shape can be adjusted to tumor size and location, while heating can be established in short time span and maintained up to 1 h with a precision of ca. 1°. The need for a tight temperature control required near real-time temperature mapping with feedback to the hyperthermia device. MR-HIFU is on its way to become a technology platform that can meet the above requirements for several hyperthermia applications. Further developments are required to generate stable and regional hyperthermia in clinically relevant tumor volumes to provide a solution for larger volume hyperthermia. Classical phased array RF-based hyperthermia is on the other hand well established for larger volume hyperthermia, and developments are ongoing for more precise and local heating. It can be expected that RF-based approaches and MR-HIFU will be complementary and have to be chosen based on patient stratification, tumor type, size and location. Industry should enable the availability of the technology and make sure it is at the adequate level (*i.e.* stable during the duration of a clinical trial).
- *Chemistry*: The current LTSL formulation based on DSPC, MSPC, and DSPE-PEG2000 is farthest developed and has reached first clinical testing in humans. However, their properties could still be improved, providing higher plasma levels of the parent drug (less leakage at body temperature, reduced clearance of LTSL) while maintaining fast release at mild hyperthermia. Both improvements would translate into higher drug levels in the target tissue and could also increase timing flexibilities in the clinical workflow. Mathematical simulations as discussed above give good guidelines in the design of these systems also to avoid large effort for incremental improvements. Furthermore, new TSLs with different parent drugs than doxorubicin are highly warranted tailored to the targeted tumor. Formulations for image-guided drug delivery showed their value in preclinical research and may offer a more personalized treatment approach for humans. However, complications arise in their compatibility with PRFS-based MR thermometry as the MRI contrast agents disturb the MR signals currently used for temperature mapping. Here, the MR community is challenged to find adequate correction methods.
- *Protocols*: Many preclinical studies used a single treatment to assess biodistribution and effects on tumor growth establishing a proof of principle. A recent preclinical study demonstrated that multiple HIFU-mediated drug delivery treatments offer improved treatment efficacy. Additional preclinical research should be devoted to develop optimal treatment protocols that are realistic for later clinical application. As a thermal therapy platform, MR-HIFU offers the unique opportunity of combining ablation and hyperthermia with radio- or systemic chemotherapy, or for temperature-triggered drug delivery, which could lead to new patient-tailored treatment options. Thus, protocol development should receive considerable attention in the coming years.
- *Applications*: Temperature-induced drug delivery using MR-HIFU has to compete with other local treatment options such as RF-ablation, external radiotherapy, and embolization techniques. The clinical community is asked to provide input and advice which patient group would benefit most from temperature-induced drug delivery. As mentioned above, MR-HIFU is a platform technology for thermal therapies that can serve an application in a more versatile way than with a local drug delivery approach only.
- *Funding*: Much research funds went into the development of the building blocks for temperature-induced drug delivery. Still, continuous effort is needed for improving the hyperthermia technology and

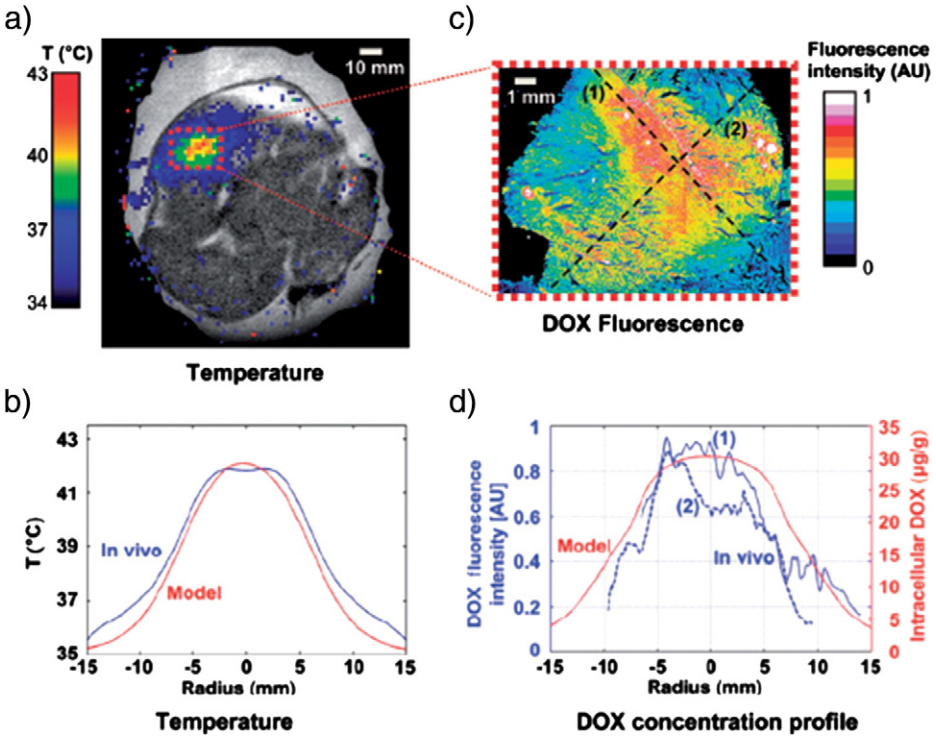

Fig. 12. (a) Temperature map during hyperthermia measured *via* MR thermometry, overlaid on pre-procedural proton density-weighted coronal image of rabbit thigh muscle. (b) Radial temperature profile (time-averaged over hyperthermia duration) from *in vivo* study (blue), compared to model (red). Profile location in model was chosen such that it traversed the maximum temperature point. Temperature deviation between simulation and *in vivo* study was 0.54 °C (mean over 15 mm radius). (c) Doxorubicin distribution measured *via* fluorescence microscopy in extracted tissue sample. (d) Doxorubicin fluorescence profile (blue) in two orthogonal directions (dashed lines marked (1) and (2) in (c), compared to doxorubicin concentration profile from computer model (red).
Reprinted with permission from Informa UK Ltd. [150].

the development of new TSL formulations. For clinical translation, extra funding should be available for upscaling, toxicity studies, and GMP production of newly formulated TSLs. However, with the disjoint business models between engineering and large pharmaceutical companies, the step to fund and execute the required large clinical studies is often considered too risky with different parties managing the study elements. Yet, a controlled study is needed to prove that the best of both worlds can revolutionize certain oncology treatments. This is best served in the setting of public private partnerships between the academia and companies in which governmental resources play a pivotal role. Public support of clinical trials would catalyze clinical translation, while keeping a strong eye on the public needs for patients at stake.

References

[1] C.L. Sawyers, Perspective: combined forces, Nature 498 (2013) S7.
[2] T.M. Allen, P.R. Cullis, Drug delivery systems: entering the mainstream, Science 303 (2004) 1818–1822.
[3] M. Ferrari, Cancer nanotechnology: opportunities and challenges, Nat. Rev. Cancer 5 (2005) 161–171.
[4] V. Wagner, A. Dullaart, A.K. Bock, A. Zweck, The emerging nanomedicine landscape, Nat. Biotechnol. 24 (2006) 1211–1217.
[5] W.R. Sanhai, J.H. Sakamoto, R. Canady, M. Ferrari, Seven challenges for nanomedicine, Nat. Nanotechnol. 3 (2008) 242–244.
[6] S. Parveen, R. Misra, S.K. Sahoo, Nanoparticles: a boon to drug delivery, therapeutics, diagnostics and imaging, Nanomedicine 8 (2012) 147–166.
[7] P.K. Working, M.S. Newman, S.K. Huang, E. Mayhew, J. Vaage, D.D. Lasic, Pharmacokinetics, biodistribution and therapeutic efficacy of doxorubicin encapsulated in Stealth® liposomes (Doxil®), J. Liposome Res. 4 (1994) 667–687.
[8] S.A. Abraham, D.N. Waterhouse, L.D. Mayer, P.R. Cullis, T.D. Madden, M.B. Bally, The liposomal formulation of doxorubicin, Methods Enzymol. 391 (2005) 71–97.
[9] H.I. Chang, M.K. Yeh, Clinical development of liposome-based drugs: formulation, characterization, and therapeutic efficacy, Int. J. Nanomedicine 7 (2012) 49–60.
[10] Y. Matsumura, H. Maeda, A new concept for macromolecular therapeutics in cancer chemotherapy: mechanism of tumoritropic accumulation of proteins and the antitumor agent smancs, Cancer Res. 46 (1986) 6387–6392.
[11] N.Z. Wu, D. Da, T.L. Rudoll, D. Needham, A.R. Whorton, M.W. Dewhirst, Increased microvascular permeability contributes to preferential accumulation of Stealth liposomes in tumor tissue, Cancer Res. 53 (1993) 3765–3770.
[12] H. Maeda, Tumor-selective delivery of macromolecular drugs via the EPR effect: background and future prospects, Bioconjug. Chem. 21 (2010) 797–802.
[13] H. Maeda, Macromolecular therapeutics in cancer treatment: the EPR effect and beyond, J. Control. Release 164 (2012) 138–144.
[14] J.A. Nagy, L. Benjamin, H. Zeng, A.M. Dvorak, H.F. Dvorak, Vascular permeability, vascular hyperpermeability and angiogenesis, Angiogenesis 11 (2008) 109–119.
[15] P. Carmeliet, R.K. Jain, Molecular mechanisms and clinical applications of angiogenesis, Nature 473 (2011) 298–307.
[16] A.K. Iyer, G. Khaled, J. Fang, H. Maeda, Exploiting the enhanced permeability and retention effect for tumor targeting, Drug Discov. Today 11 (2006) 812–818.
[17] F. Danhier, O. Feron, V. Preat, To exploit the tumor microenvironment: passive and active tumor targeting of nanocarriers for anti-cancer drug delivery, J. Control. Release 148 (2010) 135–146.
[18] H. Maeda, H. Nakamura, J. Fang, The EPR effect for macromolecular drug delivery to solid tumors: improvement of tumor uptake, lowering of systemic toxicity, and distinct tumor imaging in vivo, Adv. Drug Deliv. Rev. 65 (2013) 71–79.
[19] T. Lammers, F. Kiessling, W.E. Hennink, G. Storm, Drug targeting to tumors: principles, pitfalls and (pre-)clinical progress, J. Control. Release 161 (2012) 175–187.
[20] M.B. Yatvin, J.N. Weinstein, W.H. Dennis, R. Blumenthal, Design of liposomes for enhanced local release of drugs by hyperthermia, Science 202 (1978) 1290–1293.
[21] J.N. Weinstein, R.L. Magin, M.B. Yatvin, D.S. Zaharko, Liposomes and local hyperthermia: selective delivery of methotrexate to heated tumors, Science 204 (1979) 188–191.
[22] C. Landon, J.Y. Park, D. Needham, M.W. Dewhirst, Nanoscale drug delivery and hyperthermia: the materials design and preclinical and clinical testing of low temperature sensitive liposomes used in combination with mild hypertheria in the treatment of local cancer, Open Nanomedicine J. 3 (2011) 38–64.
[23] ClinicalTrials.gov, Phase 1/2 Study of ThermoDox™ With Approved Hyperthermia in Treatment of Breast Cancer Recurrence at the Chest Wall; 2009.
[24] ClinicalTrials.gov, A Study of ThermoDox™ in Combination with Radiofrequency Ablation (RFA) in Primary and Metastatic Tumors of the Liver; 2007.
[25] ClinicalTrials.gov, Phase 3 Study of ThermoDox™ with Radiofrequency Ablation (RFA) in Treatment of Hepatocellular Carcinoma (HCC); 2008.
[26] R.T. Poon, N. Borys, Lyso-thermosensitive liposomal doxorubicin: a novel approach to enhance efficacy of thermal ablation of liver cancer, Expert. Opin. Pharmacother. 10 (2009) 333–343.
[27] B.J. Wood, R.T. Poon, J.K. Locklin, M.R. Dreher, K.K. Ng, M. Eugeni, G. Seidel, S. Dromi, Z. Neeman, M. Kolf, C.D. Black, R. Prabhakar, S.K. Libutti, Phase I study of heat-deployed liposomal doxorubicin during radiofrequency ablation for hepatic malignancies, J. Vasc. Interv. Radiol. 23 (2012) 248–255(e247).

[28] R.W. Habash, R. Bansal, D. Krewski, H.T. Alhafid, Thermal therapy, part 2: hyperthermia techniques, Crit. Rev. Biomed. Eng. 34 (2006) 491–542.
[29] T. Helmberger, L. Marti-Bonmati, P. Pereira, A. Gillams, J. Martinez, J. Lammer, K. Malagari, A. Gangi, T. de Baere, E.J. Adam, C. Rasch, V. Budach, J.A. Reekers, Radiologists' leading position in image-guided therapy, Insights Imag. 4 (2013) 1–7.
[30] H.E. Cline, K. Hynynen, C.J. Hardy, R.D. Watkins, J.F. Schenck, F.A. Jolesz, MR temperature mapping of focused ultrasound surgery, Magn. Reson. Med. 31 (1994) 628–636.
[31] N.J. McDannold, R.L. King, F.A. Jolesz, K.H. Hynynen, Usefulness of MR imaging-derived thermometry and dosimetry in determining the threshold for tissue damage induced by thermal surgery in rabbits, Radiology 216 (2000) 517–523.
[32] J. Gellermann, B. Hildebrandt, R. Issels, H. Ganter, W. Wlodarczyk, V. Budach, R. Felix, P.U. Tunn, P. Reichardt, P. Wust, Noninvasive magnetic resonance thermography of soft tissue sarcomas during regional hyperthermia: correlation with response and direct thermometry, Cancer 107 (2006) 1373–1382.
[33] V.L. Stakhursky, O. Arabe, K.S. Cheng, J. Macfall, P. Maccarini, O. Craciunescu, M. Dewhirst, P. Stauffer, S.K. Das, Real-time MRI-guided hyperthermia treatment using a fast adaptive algorithm, Phys. Med. Biol. 54 (2009) 2131–2145.
[34] L. Ludemann, W. Wlodarczyk, J. Nadobny, M. Weihrauch, J. Gellermann, P. Wust, Non-invasive magnetic resonance thermography during regional hyperthermia, Int. J. Hyperthermia 26 (2010) 273–282.
[35] K. Hynynen, MRI-guided focused ultrasound treatments, Ultrasonics 50 (2010) 221–229.
[36] E.A. Stewart, Uterine fibroids, Lancet 357 (2001) 293–298.
[37] J. Hindley, W.M. Gedroyc, L. Regan, E. Stewart, C. Tempany, K. Hynyen, N. McDannold, Y. Inbar, Y. Itzchak, J. Rabinovici, H.S. Kim, J.F. Geschwind, G. Hesley, B. Gostout, T. Ehrenstein, S. Hengst, M. Sklair-Levy, A. Shushan, F. Jolesz, MRI guidance of focused ultrasound therapy of uterine fibroids: early results, AJR Am. J. Roentgenol. 183 (2004) 1713–1719.
[38] Y.S. Kim, H.K. Lim, J.H. Kim, H. Rhim, B.K. Park, B. Keserci, M.O. Kohler, D.S. Bae, B.G. Kim, J.W. Lee, T.J. Kim, S. Sokka, J.H. Lee, Dynamic contrast-enhanced magnetic resonance imaging predicts immediate therapeutic response of magnetic resonance-guided high-intensity focused ultrasound ablation of symptomatic uterine fibroids, Invest. Radiol. 46 (2011) 639–647.
[39] M.J. Voogt, H. Trillaud, Y.S. Kim, W.P. Mali, J. Barkhausen, L.W. Bartels, R. Deckers, N. Frulio, H. Rhim, H.K. Lim, T. Eckey, H.J. Nieminen, C. Mougenot, B. Keserci, J. Soini, T. Vaara, M.O. Kohler, S. Sokka, M.A. van den Bosch, Volumetric feedback ablation of uterine fibroids using magnetic resonance-guided high intensity focused ultrasound therapy, Eur. Radiol. 22 (2012) 411–417.
[40] A. Napoli, M. Anzidei, B.C. Marincola, G. Brachetti, F. Ciolina, G. Cartocci, C. Marsecano, F. Zaccagna, L. Marchetti, E. Cortesi, C. Catalano, Primary pain palliation and local tumor control in bone metastases treated with magnetic resonance-guided focused ultrasound, Invest. Radiol. 48 (2013) 351–358.
[41] N. Lipsman, M.L. Schwartz, Y. Huang, L. Lee, T. Sankar, M. Chapman, K. Hynynen, A.M. Lozano, MR-guided focused ultrasound thalamotomy for essential tremor: a proof-of-concept study, Lancet Neurol. 12 (2013) 462–468.
[42] P.E. Huber, J.W. Jenne, R. Rastert, I. Simiantonakis, H.P. Sinn, H.J. Strittmatter, D. von Fournier, M.F. Wannenmacher, J. Debus, A new noninvasive approach in breast cancer therapy using magnetic resonance imaging-guided focused ultrasound surgery, Cancer Res. 61 (2001) 8441–8447.
[43] R. Chopra, A. Colquhoun, M. Burtnyk, A. N'Djin, W.I. Kobelevskiy, A. Boyes, K. Siddiqui, H. Foster, L. Sugar, M.A. Haider, M. Bronskill, L. Klotz, MR imaging-controlled transurethral ultrasound therapy for conformal treatment of prostate tissue: initial feasibility in humans, Radiology 265 (2012) 303–313.
[44] G.M. Hahn, Hyperthermia and Cancer, Plenum Press, New York, 1982.
[45] M.R. Horsman, J. Overgaard, Hyperthermia: a potent enhancer of radiotherapy, Clin. Oncol. (R. Coll. Radiol.) 19 (2007) 418–426.
[46] J.L. Roti Roti, Introduction: radiosensitization by hyperthermia, Int. J. Hyperthermia 20 (2004) 109–114.
[47] M.W. Dewhirst, Z. Vujaskovic, E. Jones, D. Thrall, Re-setting the biologic rationale for thermal therapy, Int. J. Hyperthermia 21 (2005) 779–790.
[48] R.D. Issels, Hyperthermia adds to chemotherapy, Eur. J. Cancer 44 (2008) 2546–2554.
[49] J.L. Roti Roti, Cellular responses to hyperthermia (40–46 °C): cell killing and molecular events, Int. J. Hyperthermia 24 (2008) 3–15.
[50] G. Baronzio, I. Freitas, P. Griffini, V. Bertone, F. Pacini, G. Mascaro, E. Razzini, A. Gramaglia, Omega-3 fatty acids can improve radioresponse modifying tumor interstitial pressure, blood rheology and membrane peroxidability, Anticancer Res. 14 (1994) 1145–1154.
[51] G. Kong, R.D. Braun, M.W. Dewhirst, Characterization of the effect of hyperthermia on nanoparticle extravasation from tumor vasculature, Cancer Res. 61 (2001) 3027–3032.
[52] J. Overgaard, D. Gonzalez Gonzalez, M.C. Hulshof, G. Arcangeli, O. Dahl, O. Mella, S.M. Bentzen, Hyperthermia as an adjuvant to radiation therapy of recurrent or metastatic malignant melanoma. A multicentre randomized trial by the European Society for Hyperthermic Oncology, Int. J. Hyperthermia 12 (1996) 3–20.
[53] R. de Wit, J. van der Zee, M.E. van der Burg, W.H. Kruit, A. Logmans, G.C. van Rhoon, J. Verweij, A phase I/II study of combined weekly systemic cisplatin and locoregional hyperthermia in patients with previously irradiated recurrent carcinoma of the uterine cervix, Br. J. Cancer 80 (1999) 1387–1391.
[54] J. van der Zee, G.C. van Rhoon, Cervical cancer: radiotherapy and hyperthermia, Int. J. Hyperthermia 22 (2006) 229–234.
[55] M. Franckena, D. Fatehi, M. de Bruijne, R.A. Canters, Y. van Norden, J.W. Mens, G.C. van Rhoon, J. van der Zee, Hyperthermia dose–effect relationship in 420 patients with cervical cancer treated with combined radiotherapy and hyperthermia, Eur. J. Cancer 45 (2009) 1969–1978.
[56] R.D. Issels, L.H. Lindner, J. Verweij, P. Wust, P. Reichardt, B.C. Schem, S. Abdel-Rahman, S. Daugaard, C. Salat, C.M. Wendtner, Z. Vujaskovic, R. Wessalowski, K.W. Jauch, H.R. Durr, F. Ploner, A. Baur-Melnyk, U. Mansmann, W. Hiddemann, J.Y. Blay, P. Hohenberger, Neo-adjuvant chemotherapy alone or with regional hyperthermia for localised high-risk soft-tissue sarcoma: a randomised phase 3 multicentre study, Lancet Oncol. 11 (2010) 561–570.
[57] J.R. Oleson, T.V. Samulski, K.A. Leopold, S.T. Clegg, M.W. Dewhirst, R.K. Dodge, S.L. George, Sensitivity of hyperthermia trial outcomes to temperature and time: implications for thermal goals of treatment, Int. J. Radiat. Oncol. Biol. Phys. 25 (1993) 289–297.
[58] D.S. Kapp, R.S. Cox, Thermal treatment parameters are most predictive of outcome in patients with single tumor nodules per treatment field in recurrent adenocarcinoma of the breast, Int. J. Radiat. Oncol. Biol. Phys. 33 (1995) 887–899.
[59] M. Sherar, F.F. Liu, M. Pintilie, W. Levin, J. Hunt, R. Hill, J. Hand, C. Vernon, G. van Rhoon, J. van der Zee, D.G. Gonzalez, J. van Dijk, J. Whaley, D. Machin, Relationship between thermal dose and outcome in thermoradiotherapy treatments for superficial recurrences of breast cancer: data from a phase III trial, Int. J. Radiat. Oncol. Biol. Phys. 39 (1997) 371–380.
[60] D.E. Thrall, S.M. LaRue, D. Yu, T. Samulski, L. Sanders, B. Case, G. Rosner, C. Azuma, J. Poulson, A.F. Pruitt, W. Stanley, M.L. Hauck, L. Williams, P. Hess, M.W. Dewhirst, Thermal dose is related to duration of local control in canine sarcomas treated with thermoradiotherapy, Clin. Cancer Res. 11 (2005) 5206–5214.
[61] E. Jones, D. Thrall, M.W. Dewhirst, Z. Vujaskovic, Prospective thermal dosimetry: the key to hyperthermia's future, Int. J. Hyperthermia 22 (2006) 247–253.
[62] C.W. Song, Effect of local hyperthermia on blood flow and microenvironment: a review, Cancer Res. 44 (1984) 4721s–4730s.
[63] P.W. Vaupel, D.K. Kelleher, Pathophysiological and vascular characteristics of tumours and their importance for hyperthermia: heterogeneity is the key issue, Int. J. Hyperthermia 26 (2010) 211–223.
[64] J.G. Lynn, R.L. Zwemer, A.J. Chick, The biological application of focused ultrasonic waves, Science 96 (1942) 119–120.
[65] H.E. Cline, J.F. Schenck, R.D. Watkins, K. Hynynen, F.A. Jolesz, Magnetic resonance-guided thermal surgery, Magn. Reson. Med. 30 (1993) 98–106.
[66] K. Hynynen, W.R. Freund, H.E. Cline, A.H. Chung, R.D. Watkins, J.P. Vetro, F.A. Jolesz, A clinical, noninvasive, MR imaging-monitored ultrasound surgery method, Radiographics 16 (1996) 185–195.
[67] K. Hynynen, MRIgHIFU: a tool for image-guided therapeutics, J. Magn. Reson. Imaging 34 (2011) 482–493.
[68] W.C. Dewey, Arrhenius relationships from the molecule and cell to the clinic, Int. J. Hyperthermia 25 (2009) 3–20.
[69] G. ter Haar, D. Sinnett, I. Rivens, High intensity focused ultrasound—a surgical technique for the treatment of discrete liver tumours, Phys. Med. Biol. 34 (1989) 1743–1750.
[70] K. Hynynen, The threshold for thermally significant cavitation in dog's thigh muscle in vivo, Ultrasound Med. Biol. 17 (1991) 157–169.
[71] G.T. Haar, C. Coussios, High intensity focused ultrasound: past, present and future, Int. J. Hyperthermia 23 (2007) 85–87.
[72] Y. Ishihara, A. Calderon, H. Watanabe, K. Okamoto, Y. Suzuki, K. Kuroda, Y. Suzuki, A precise and fast temperature mapping using water proton chemical shift, Magn. Reson. Med. 34 (1995) 814–823.
[73] McDannold, K. Hynynen, D. Wolf, G. Wolf, F. Jolesz, MRI evaluation of thermal ablation of tumors with focused ultrasound, J. Magn. Reson. Imaging 8 (1998) 91–100.
[74] V. Rieke, K. Butts Pauly, MR thermometry, J. Magn. Reson. Imaging 27 (2008) 376–390.
[75] B. Denis de Senneville, B. Quesson, C.T. Moonen, Magnetic resonance temperature imaging, Int. J. Hyperthermia 21 (2005) 515–531.
[76] A. Kickhefel, J. Roland, C. Weiss, F. Schick, Accuracy of real-time MR temperature mapping in the brain: a comparison of fast sequences, Phys. Med. 26 (2010) 192–201.
[77] D. Schlesinger, S. Benedict, C. Diederich, W. Gedroyc, A. Klibanov, J. Larner, MR-guided focused ultrasound surgery, present and future, Med. Phys. 40 (2013) 080901.
[78] D.R. Daum, K. Hynynen, A 256-element ultrasonic phased array system for the treatment of large volumes of deep seated tissue, IEEE Trans. Ultrason. Ferroelectr. Freq. Control 46 (1999) 1254–1268.
[79] G.T. Haar, C. Coussios, High intensity focused ultrasound: physical principles and devices, Int. J. Hyperthermia 23 (2007) 89–104.
[80] X. Fan, K. Hynynen, Ultrasound surgery using multiple sonications—treatment time considerations, Ultrasound Med. Biol. 22 (1996) 471–482.
[81] M.O. Köhler, C. Mougenot, B. Quesson, J. Enholm, B. Le Bail, C. Laurent, C.T. Moonen, G.J. Ehnholm, Volumetric HIFU ablation under 3D guidance of rapid MRI thermometry, Med. Phys. 36 (2009) 3521–3535.
[82] E.S. Ebbini, S.I. Umemura, M. Ibbini, C.A. Cain, A cylindrical-section ultrasound phased-array applicator for hyperthermia cancer therapy, IEEE Trans. Ultrason. Ferroelectr. Freq. Control 35 (1988) 561–572.
[83] N.M. Hijnen, E. Heijman, M.O. Kohler, M. Ylihautala, G.J. Ehnholm, A.W. Simonetti, H. Grull, Tumour hyperthermia and ablation in rats using a clinical MR-HIFU system equipped with a dedicated small animal set-up, Int. J. Hyperthermia 28 (2012) 141–155.
[84] J.K. Enholm, M.O. Köhler, B. Quesson, C. Mougenot, C.T. Moonen, S.D. Sokka, Improved volumetric MR-HIFU ablation by robust binary feedback control, IEEE Trans. Biomed. Eng. 57 (2010) 103–113.
[85] M. de Smet, E. Heijman, S. Langereis, N.M. Hijnen, H. Grull, Magnetic resonance imaging of high intensity focused ultrasound mediated drug delivery from temperature-sensitive liposomes: an in vivo proof-of-concept study, J. Control. Release 150 (2011) 102–110.

[86] A. Ranjan, G.C. Jacobs, D.L. Woods, A.H. Negussie, A. Partanen, P.S. Yarmolenko, C.E. Gacchina, K.V. Sharma, V. Frenkel, B.J. Wood, M.R. Dreher, Image-guided drug delivery with magnetic resonance guided high intensity focused ultrasound and temperature sensitive liposomes in a rabbit Vx2 tumor model, J. Control. Release 158 (3) (2011) 487–494.
[87] A. Partanen, P.S. Yarmolenko, A. Viitala, S. Appanaboyina, D. Haemmerich, A. Ranjan, G. Jacobs, D. Woods, J. Enholm, B.J. Wood, M.R. Dreher, Mild hyperthermia with magnetic resonance-guided high-intensity focused ultrasound for applications in drug delivery, Int. J. Hyperthermia 28 (2012) 320–336.
[88] A. Ranjan, G.C. Jacobs, D.L. Woods, A.H. Negussie, A. Partanen, P.S. Yarmolenko, C.E. Gacchina, K.V. Sharma, V. Frenkel, B.J. Wood, M.R. Dreher, Image-guided drug delivery with magnetic resonance guided high intensity focused ultrasound and temperature sensitive liposomes in a rabbit Vx2 tumor model, J. Control. Release 158 (2012) 487–494.
[89] A. Partanen, M. Tillander, P.S. Yarmolenko, B.J. Wood, M.R. Dreher, M.O. Kohler, Reduction of peak acoustic pressure and shaping of heated region by use of multifoci sonications in MR-guided high-intensity focused ultrasound mediated mild hyperthermia, Med. Phys. 40 (2013) 013301.
[90] D. Marsh, Handbook of Lipid Bilayers, CRC Press, 1990.
[91] G. Kong, G. Anyarambhatla, W.P. Petros, R.D. Braun, O.M. Colvin, D. Needham, M.W. Dewhirst, Efficacy of liposomes and hyperthermia in a human tumor xenograft model: importance of triggered drug release, Cancer Res. 60 (2000) 6950–6957.
[92] D. Needham, G. Anyarambhatla, G. Kong, M.W. Dewhirst, A new temperature-sensitive liposome for use with mild hyperthermia: characterization and testing in a human tumor xenograft model, Cancer Res. 60 (2000) 1197–1201.
[93] P.S. Yarmolenko, Y. Zhao, C. Landon, I. Spasojevic, F. Yuan, D. Needham, B.L. Viglianti, M.W. Dewhirst, Comparative effects of thermosensitive doxorubicin-containing liposomes and hyperthermia in human and murine tumours, Int. J. Hyperthermia 26 (2010) 485–498.
[94] D. Needham, J.-Y. Park, A.M. Wright, J. Tong, Materials characterization of the low temperature sensitive liposome (LTSL): effects of the lipid composition (lysolipid and DSPE-PEG2000) on the thermal transition and release of doxorubicin, Faraday Discuss. 161 (2013) 515–534.
[95] G.R. Anyarambhatla, D. Needham, Enhancement of the phase transition permeability of DPPC liposomes by incorporation of MPPC: a new temperature-sensitive liposome for use with mild hyperthermia, J. Liposome Res. 9 (1999) 491–506.
[96] D. Needham, M.W. Dewhirst, The development and testing of a new temperature-sensitive drug delivery system for the treatment of solid tumors, Adv. Drug Deliv. Rev. 53 (2001) 285–305.
[97] L.M. Ickenstein, K. Edwards, G. Karlsson, L.D. Mayer, Formation of bilayer discs in lysolipid-containing thermosensitive liposomes during phase transition: a new drug release mechanism, J. Liposome Res. 13 (2003) 39–40.
[98] M.C. Sandstrom, L.M. Ickenstein, L.D. Mayer, K. Edwards, Effects of lipid segregation and lysolipid dissociation on drug release from thermosensitive liposomes, J. Control. Release 107 (2005) 131–142.
[99] A.L. Klibanov, K. Maruyama, V.P. Torchilin, L. Huang, Amphipathic polyethyleneglycols effectively prolong the circulation time of liposomes, FEBS Lett. 268 (1990) 235–237.
[100] J.K. Mills, D. Needham, Lysolipid incorporation in dipalmitoylphosphatidylcholine bilayer membranes enhances the ion permeability and drug release rates at the membrane phase transition, Biochim. Biophys. Acta Biomembr. 1716 (2005) 77–96.
[101] L.H. Lindner, M.E. Eichhorn, H. Eibl, N. Teichert, M. Schmitt-Sody, R.D. Issels, M. Dellian, Novel temperature-sensitive liposomes with prolonged circulation time, Clin. Cancer Res. 10 (2004) 2168–2178.
[102] M. Hossann, M. Wiggenhorn, A. Schwerdt, K. Wachholz, N. Teichert, H. Eibl, R.D. Issels, L.H. Lindner, In vitro stability and content release properties of phosphatidylglyceroglycerol containing thermosensitive liposomes, Biochim. Biophys. Acta 1768 (2007) 2491–2499.
[103] T. Tagami, M.J. Ernsting, S.D. Li, Optimization of a novel and improved thermosensitive liposome formulated with DPPC and a Brij surfactant using a robust in vitro system, J. Control. Release 154 (2011) 290–297.
[104] S.M. Park, M.S. Kim, S.J. Park, E.S. Park, K.S. Choi, Y.S. Kim, H.R. Kim, Novel temperature-triggered liposome with high stability: formulation, in vitro evaluation, and in vivo study combined with high-intensity focused ultrasound (HIFU), J. Control. Release 170 (2013) 373–379.
[105] M.R. Dreher, D. Raucher, N. Balu, O.M. Colvin, S.M. Ludeman, A. Chilkoti, Evaluation of an elastin-like polypeptide–doxorubicin conjugate for cancer therapy, J. Control. Release 91 (2003) 31–43.
[106] S.A. Abraham, K. Edwards, G. Karlsson, S. MacIntosh, L.D. Mayer, C. McKenzie, M.B. Bally, Formation of transition metal–doxorubicin complexes inside liposomes, Biochim. Biophys. Acta 1565 (2002) 41–54.
[107] B.L. Viglianti, S.A. Abraham, C.R. Michelich, P.S. Yarmolenko, J.R. MacFall, M.B. Bally, M.W. Dewhirst, In vivo monitoring of tissue pharmacokinetics of liposome/drug using MRI: illustration of targeted delivery, Magn. Reson. Med. 51 (2004) 1153–1162.
[108] A. Kheirolomoom, C.Y. Lai, S.M. Tam, L.M. Mahakian, E.S. Ingham, K.D. Watson, K.W. Ferrara, Complete regression of local cancer using temperature-sensitive liposomes combined with ultrasound-mediated hyperthermia, J. Control. Release 172 (2013) 266–273.
[109] V.J. Caride, H.D. Sostman, R.J. Winchell, J.C. Gore, Relaxation enhancement using liposomes carrying paramagnetic species, Magn. Reson. Imaging 2 (1984) 107–112.
[110] R.L. Magin, S.M. Wright, M.R. Niesman, H.C. Chan, H.M. Swartz, Liposome delivery of NMR contrast agents for improved tissue imaging, Magn. Reson. Med. 3 (1986) 440–447.
[111] J.M. Devoisselle, J. Vion-Dury, J.P. Galons, S. Confort-Gouny, D. Coustaut, P. Canioni, P.J. Cozzone, Entrapment of gadolinium-DTPA in liposomes. Characterization of vesicles by P-31 NMR spectroscopy, Invest. Radiol. 23 (1988) 719–724.
[112] E. Unger, P. Needleman, P. Cullis, C. Tilcock, Gadolinium-DTPA liposomes as a potential MRI contrast agent. Work in progress, Invest. Radiol. 23 (1988) 928–932.
[113] S. Langereis, T. Geelen, H. Grull, G.J. Strijkers, K. Nicolay, Paramagnetic liposomes for molecular MRI and MRI-guided drug delivery, NMR Biomed. 26 (2013) 728–744.
[114] E. Terreno, D.D. Castelli, A. Viale, S. Aime, Challenges for molecular magnetic resonance imaging, Chem. Rev. 110 (2010) 3019–3042.
[115] D.D. Castelli, E. Terreno, D. Longo, S. Aime, Nanoparticle-based chemical exchange saturation transfer (CEST) agents, NMR Biomed. 26 (2013) 839–849.
[116] G. Bacic, M.R. Niesman, H.F. Bennett, R.L. Magin, H.M. Swartz, Modulation of water proton relaxation rates by liposomes containing paramagnetic materials, Magn. Reson. Med. 6 (1988) 445–458.
[117] C. Tilcock, E. Unger, P. Cullis, P. MacDougall, Liposomal Gd-DTPA: preparation and characterization of relaxivity, Radiology 171 (1989) 77–80.
[118] S.H. Koenig, Q.F. Ahkong, R.D. Brown III, M. Lafleur, M. Spiller, E. Unger, C. Tilcock, Permeability of liposomal membranes to water: results from the magnetic field dependence of T1 of solvent protons in suspensions of vesicles with entrapped paramagnetic ions, Magn. Reson. Med. 23 (1992) 275–286.
[119] S.L. Fossheim, K.A. Il'yasov, J. Hennig, A. Bjornerud, Thermosensitive paramagnetic liposomes for temperature control during MR imaging-guided hyperthermia: in vitro feasibility studies, Acad. Radiol. 7 (2000) 1107–1115.
[120] J.A. de Zwart, R. Salomir, F. Vimeux, J. Klaveness, C.T.W. Moonen, On the feasibility of local drug delivery using thermo-sensitive liposomes and MR-guided focused ultrasound, Proc. Int. Soc. Magn. Reson. Med. 8 (2000).
[121] N. McDannold, S.L. Fossheim, H. Rasmussen, H. Martin, N. Vykhodtseva, K. Hynynen, Heat-activated liposomal MR contrast agent: initial in vivo results in rabbit liver and kidney, Radiology 230 (2004) 743–752.
[122] T. Wang, M. Hossann, H.M. Reinl, M. Peller, H. Eibl, M. Reiser, R.D. Issels, L.H. Lindner, In vitro characterization of phosphatidylglyceroglycerol-based thermosensitive liposomes with encapsulated ^{1}H MR T1-shortening gadodiamide, Contrast Media Mol. Imaging 3 (2008) 19–26.
[123] M. Peller, A. Schwerdt, M. Hossann, H.M. Reinl, T. Wang, S. Sourbron, M. Ogris, L.H. Lindner, MR characterization of mild hyperthermia-induced gadodiamide release from thermosensitive liposomes in solid tumors, Invest. Radiol. 43 (2008) 877–892.
[124] M. Hossann, T. Wang, Z. Syunyaeva, M. Wiggenhorn, A. Zengerle, R.D. Issels, M. Reiser, L.H. Lindner, M. Peller, Non-ionic Gd-based MRI contrast agents are optimal for encapsulation into phosphatidyldiglycerol-based thermosensitive liposomes, J. Control. Release 166 (2013) 22–29.
[125] B.L. Viglianti, A.M. Ponce, C.R. Michelich, D. Yu, S.A. Abraham, L. Sanders, P.S. Yarmolenko, T. Schroeder, J.R. MacFall, D.P. Barboriak, O.M. Colvin, M.B. Bally, M.W. Dewhirst, Chemodosimetry of in vivo tumor liposomal drug concentration using MRI, Magn. Reson. Med. 56 (2006) 1011–1018.
[126] M. de Smet, S. Langereis, S. van den Bosch, H. Grull, Temperature-sensitive liposomes for doxorubicin delivery under MRI guidance, J. Control. Release 143 (2010) 120–127.
[127] A.H. Negussie, P.S. Yarmolenko, A. Partanen, A. Ranjan, G. Jacobs, D. Woods, H. Bryant, D. Thomasson, M.W. Dewhirst, B.J. Wood, M.R. Dreher, Formulation and characterisation of magnetic resonance imageable thermally sensitive liposomes for use with magnetic resonance-guided high intensity focused ultrasound, Int. J. Hyperthermia 27 (2011) 140–155.
[128] T. Tagami, W.D. Foltz, M.J. Ernsting, C.M. Lee, I.F. Tannock, J.P. May, S.D. Li, MRI monitoring of intratumoral drug delivery and prediction of the therapeutic effect with a multifunctional thermosensitive liposome, Biomaterials 32 (2011) 6570–6578.
[129] S. Langereis, J. Keupp, J.L. van Velthoven, I.H. de Roos, D. Burdinski, J.A. Pikkemaat, H. Grull, A temperature-sensitive liposomal ^{1}H CEST and ^{19}F contrast agent for MR image-guided drug delivery, J. Am. Chem. Soc. 131 (2009) 1380–1381.
[130] C. Lorenzato, A. Cernicanu, M.-E. Meyre, M. Germain, A. Pottier, L. Levy, B.D. de Senneville, C. Bos, C. Moonen, MRI contrast variation of thermosensitive magnetoliposomes triggered by focused ultrasound: a tool for image-guided local drug delivery, Contrast Media Mol. Imaging 8 (2012) 185–192.
[131] L. Frich, A. Bjornerud, S. Fossheim, T. Tillung, I. Gladhaug, Experimental application of thermosensitive paramagnetic liposomes for monitoring magnetic resonance imaging guided thermal ablation, Magn. Reson. Med. 52 (2004) 1302–1309.
[132] A.M. Ponce, B.L. Viglianti, D. Yu, P.S. Yarmolenko, C.R. Michelich, J. Woo, M.B. Bally, M.W. Dewhirst, Magnetic resonance imaging of temperature-sensitive liposome release: drug dose painting and antitumor effects, J. Natl. Cancer Inst. 99 (2007) 53–63.
[133] C. Lorenzato, A. Cernicanu, M.E. Meyre, M. Germain, A. Pottier, L. Levy, B.D. de Senneville, C. Bos, C. Moonen, P. Smirnov, MRI contrast variation of thermosensitive magnetoliposomes triggered by focused ultrasound: a tool for image-guided local drug delivery, Contrast Media Mol. Imaging 8 (2013) 185–192.
[134] H. Grull, S. Langereis, Hyperthermia-triggered drug delivery from temperature-sensitive liposomes using MRI-guided high intensity focused ultrasound, J. Control. Release 161 (2012) 317–327.
[135] J.P. May, S.D. Li, Hyperthermia-induced drug targeting, Expert Opin. Drug Deliv. 10 (2013) 511–527.
[136] N.M. Hijnen, A. Elevelt, J. Pikkemaat, C. Bos, L.W. Bartels, G. H., The magnetic susceptibility effect of gadolinium-based contrast agents on PRFS-based MR thermometry during thermal interventions, J. Ther. Ultrasound 1:8 (2013).
[137] M. de Smet, N.M. Hijnen, S. Langereis, A. Elevelt, E. Heijman, L. Dubois, P. Lambin, H. Grull, Magnetic resonance guided high-intensity focused ultrasound mediated hyperthermia improves the intratumoral distribution of temperature-sensitive liposomal doxorubicin, Invest. Radiol. 48 (2013) 395–405.

[138] M. Rohrer, H. Bauer, J. Mintorovitch, M. Requardt, H.J. Weinmann, Comparison of magnetic properties of MRI contrast media solutions at different magnetic field strengths, Invest. Radiol. 40 (2005) 715–724.
[139] L. Li, T.L. ten Hagen, M. Bolkestein, A. Gasselhuber, J. Yatvin, G.C. van Rhoon, A.M. Eggermont, D. Haemmerich, G.A. Koning, Improved intratumoral nanoparticle extravasation and penetration by mild hyperthermia, J. Control. Release 167 (2013) 130–137.
[140] M. de Smet, S. Langereis, S. van den Bosch, K. Bitter, N.M. Hijnen, E. Heijman, H. Grull, SPECT/CT imaging of temperature-sensitive liposomes for MR-image guided drug delivery with high intensity focused ultrasound, J. Control. Release 169 (2013) 82–90.
[141] A.A. Manzoor, L.H. Lindner, C.D. Landon, J.Y. Park, A.J. Simnick, M.R. Dreher, S. Das, G. Hanna, W. Park, A. Chilkoti, G.A. Koning, T.L. Ten Hagen, D. Needham, M.W. Dewhirst, Overcoming limitations in nanoparticle drug delivery: triggered, intravascular release to improve drug penetration into tumors, Cancer Res. 72 (2012) 5566–5575.
[142] R.M. Staruch, M. Ganguly, I.F. Tannock, K. Hynynen, R. Chopra, Enhanced drug delivery in rabbit VX2 tumours using thermosensitive liposomes and MRI-controlled focused ultrasound hyperthermia, Int. J. Hyperthermia 28 (2012) 776–787.
[143] G.A. Koning, A.M. Eggermont, L.H. Lindner, T.L. ten Hagen, Hyperthermia and thermosensitive liposomes for improved delivery of chemotherapeutic drugs to solid tumors, Pharm. Res. 27 (2010) 1750–1754.
[144] A. Gasselhuber, M.R. Dreher, A. Negussie, B.J. Wood, F. Rattay, D. Haemmerich, Mathematical spatio-temporal model of drug delivery from low temperature sensitive liposomes during radiofrequency tumour ablation, Int. J. Hyperthermia 26 (2010) 499–513.
[145] B.D. Weinberg, R.B. Patel, A.A. Exner, G.M. Saidel, J. Gao, Modeling doxorubicin transport to improve intratumoral drug delivery to RF ablated tumors, J. Control. Release 124 (2007) 11–19.
[146] A. Gasselhuber, M.R. Dreher, F. Rattay, B.J. Wood, D. Haemmerich, Comparison of conventional chemotherapy, stealth liposomes and temperature-sensitive liposomes in a mathematical model, PLoS One 7 (2012) e47453.
[147] R. Staruch, R. Chopra, K. Hynynen, Localised drug release using MRI-controlled focused ultrasound hyperthermia, Int. J. Hyperthermia 27 (2011) 156–171.
[148] F. Yuan, M. Leunig, S.K. Huang, D.A. Berk, D. Papahadjopoulos, R.K. Jain, Microvascular permeability and interstitial penetration of sterically stabilized (stealth) liposomes in a human tumor xenograft, Cancer Res. 54 (1994) 3352–3356.
[149] A.L. Seynhaeve, S. Hoving, D. Schipper, C.E. Vermeulen, G. de Wiel-Ambagtsheer, S.T. van Tiel, A.M. Eggermont, T.L. Ten Hagen, Tumor necrosis factor alpha mediates homogeneous distribution of liposomes in murine melanoma that contributes to a better tumor response, Cancer Res. 67 (2007) 9455–9462.
[150] A. Gasselhuber, M.R. Dreher, A. Partanen, P.S. Yarmolenko, D. Woods, B.J. Wood, D. Haemmerich, Targeted drug delivery by high intensity focused ultrasound mediated hyperthermia combined with temperature-sensitive liposomes: computational modelling and preliminary in vivovalidation, Int. J. Hyperthermia 28 (2012) 337–348.
[151] ClinicalTrials.gov, Phase 3 study of ThermoDox with radiofrequency ablation (RFA) in treatment of hepatocellular carcinoma (HCC), in: M. Nicholas Borys (Ed.), 2011.
[152] S.N. Goldberg, G.D. Girnan, A.N. Lukyanov, M. Ahmed, W.L. Monsky, G.S. Gazelle, J.C. Huertas, K.E. Stuart, T. Jacobs, V.P. Torchillin, E.F. Halpern, J.B. Kruskal, Percutaneous tumor ablation: increased necrosis with combined radio-frequency ablation and intravenous liposomal doxorubicin in a rat breast tumor model, Radiology 222 (2002) 797–804.
[153] H.W. Head, G.D. Dodd III, A. Bao, A. Soundararajan, X. Garcia-Rojas, T.J. Prihoda, L.M. McManus, B.A. Goins, C.A. Santoyo, W.T. Phillips, Combination radiofrequency ablation and intravenous radiolabeled liposomal Doxorubicin: imaging and quantification of increased drug delivery to tumors, Radiology 255 (2010) 405–414.
[154] R. Lencioni, New IO Approaches for HCC: an update on clinical trials, www.Celsion.com.
[155] S. Dromi, V. Frenkel, A. Luk, B. Traughber, M. Angstadt, M. Bur, J. Poff, J. Xie, S.K. Libutti, K.C.P. Li, B.J. Wood, Pulsed-high intensity focused ultrasound and low temperature-sensitive liposomes for enhanced targeted drug delivery and antitumor effect, Clin. Cancer Res. 13 (2007) 2722–2727.
[156] P.R. Patel, A. Luk, A. Durrani, S. Dromi, J. Cuesta, M. Angstadt, M.R. Dreher, B.J. Wood, V. Frenkel, In vitro and in vivo evaluations of increased effective beam width for heat deposition using a split focus high intensity ultrasound (HIFU) transducer, Int. J. Hyperthermia 24 (2008) 537–549.
[157] R. Staruch, R. Chopra, K. Hynynen, Hyperthermia in bone generated with MR imaging-controlled focused ultrasound: control strategies and drug delivery, Radiology 263 (2012) 117–127.